Electronic Supplementary Material (ESI) for Physical Chemistry Chemical Physics.

Electronic supplementary information (ESI)

On the Formation of Complex Organic Molecules in the Interstellar Medium: Untangling the Chemical Complexity of Carbon Monoxide-Hydrocarbon Containing Analogue Ices Exposed to Ionizing Radiation via a Combined Infrared and Reflectron Time-Of-Flight Analysis

Matthew J. Abplanalp[1,2], Ralf I. Kaiser[1,2]

[1] W. M. Keck Research Laboratory in Astrochemistry, University of Hawaii at Manoa, Honolulu, HI, 96822, USA; ralfk@hawaii.edu

[2] Department of Chemistry, University of Hawaii at Manoa, Honolulu, HI, 96822, USA

*Correspondence should be addressed to Ralf I. Kaiser: ralfk@hawaii.edu

Table of Contents

Table S1. Isotopic FTIR assignments before and after irradiation…S5

Figure S1. Infrared spectra before (black) and after (red) irradiation of carbon monoxide-methane ($CO–CH_4$) ice…S9

Figure S2. Infrared spectra before (black) and after (red) irradiation of carbon monoxide-ethane ($CO–C_2H_6$) ice…S10

Figure S3. Infrared spectra before (black) and after (red) irradiation of carbon monoxide-ethylene ($CO–C_2H_4$) ice…S11

Figure S4. Infrared spectra before (black) and after (red) irradiation of carbon monoxide-acetylene ($CO–C_2H_2$) ice…S12

Figure S5. PI-ReTOF-MS ion signal for C_2H_nO (n = 2, 4, 6) versus temperature subliming from carbon monoxide-ethane ($CO–C_2H_6$; $C^{18}O–C_2H_6$) ices…S13

Figure S6. PI-ReTOF-MS ion signal for C_2H_nO (n = 2, 4, 6) versus temperature subliming from carbon monoxide-ethylene ($CO–C_2H_4$; $C^{18}O–C_2D_4$) ices…S14

Figure S7. PI-ReTOF-MS ion signal for C_2H_nO (n = 2, 4, 6) versus temperature subliming from carbon monoxide-acetylene ($CO–C_2H_2$; $C^{18}O–C_2D_2$) ices…S15

Figure S8. PI-ReTOF-MS ion signal for C_3H_nO (n = 2, 4, 6, 8) versus temperature subliming from carbon monoxide-ethane ($CO–C_2H_6$; $C^{18}O–C_2H_6$) ices…S16

Figure S9. PI-ReTOF-MS ion signal for C_3H_nO (n = 2, 4, 6, 8) versus temperature subliming from carbon monoxide-ethylene ($CO–C_2H_4$; $C^{18}O–C_2D_4$) ices…S17

Figure S10. PI-ReTOF-MS ion signal for C_3H_nO (n = 2, 4, 6, 8) versus temperature subliming from carbon monoxide-acetylene ($CO–C_2H_2$; $C^{18}O–C_2D_2$) ices…S18

Figure S11. PI-ReTOF-MS ion signal for C_4H_nO (n = 4, 6, 8, 10) versus temperature subliming from carbon monoxide-ethane ($CO–C_2H_6$; $C^{18}O–C_2H_6$) ices…S19

Figure S12. PI-ReTOF-MS ion signal for C_4H_nO (n = 4, 6, 8, 10) versus temperature subliming from carbon monoxide-ethylene ($CO–C_2H_4$; $C^{18}O–C_2D_4$) ices…S20

Figure S13. PI-ReTOF-MS ion signal for C_4H_nO (n = 4, 6, 8, 10) versus temperature subliming from carbon monoxide-acetylene ($CO–C_2H_2$; $C^{18}O–C_2D_2$) ices…S21

Figure S14. PI-ReTOF-MS ion signal for C_5H_nO (n = 4, 6, 8, 10) versus temperature subliming from carbon monoxide-ethane ($CO–C_2H_6$; $C^{18}O–C_2H_6$) ices…S22

Figure S15. PI-ReTOF-MS ion signal for C_5H_nO (n = 4, 6, 8, 10) versus temperature subliming from carbon monoxide-ethylene ($CO–C_2H_4$; $C^{18}O–C_2D_4$) ices…S23

Figure S16. PI-ReTOF-MS ion signal for C_5H_nO (n = 4, 6, 8, 10) versus temperature subliming from carbon monoxide-acetylene ($CO–C_2H_2$; $C^{18}O–C_2D_2$) ices…S24

Figure S17. PI-ReTOF-MS ion signal for C_6H_nO (n = 4, 6, 8, 10, 12, 14) versus temperature subliming from carbon monoxide-ethane ($CO–C_2H_6$; $C^{18}O–C_2H_6$) ices…S25

Figure S18. PI-ReTOF-MS ion signal for C_6H_nO (n = 4, 6, 8, 10, 12, 14) versus temperature subliming from carbon monoxide-ethylene ($CO–C_2H_4$; $C^{18}O–C_2D_4$) ices…S26

Figure S19. PI-ReTOF-MS ion signal for C_6H_nO (n = 4, 6, 8, 10, 12, 14) versus temperature subliming from carbon monoxide-acetylene ($CO–C_2H_2$; $C^{18}O–C_2D_2$) ices…S27

Figure S20. PI-ReTOF-MS ion signal for $C_2H_nO_2$ (n = 2, 4) versus temperature subliming from carbon monoxide-ethane ($CO–C_2H_6$; $C^{18}O–C_2H_6$) ices…S28

Figure S21. PI-ReTOF-MS ion signal for $C_2H_nO_2$ (n = 2, 4) versus temperature subliming from carbon monoxide-ethylene ($CO–C_2H_4$; $C^{18}O–C_2D_4$) ices…S29

Figure S22. PI-ReTOF-MS ion signal for $C_2H_nO_2$ (n = 2, 4) versus temperature subliming from carbon monoxide-acetylene ($CO–C_2H_2$; $C^{18}O–C_2D_2$) ices…S30

Figure S23. PI-ReTOF-MS ion signal for $C_3H_nO_2$ (n = 4, 6, 8) versus temperature subliming from carbon monoxide-ethane ($CO–C_2H_6$; $C^{18}O–C_2H_6$) ices…S31

Figure S24. PI-ReTOF-MS ion signal for $C_3H_nO_2$ (n = 4, 6, 8) versus temperature subliming from carbon monoxide-ethylene ($CO–C_2H_4$; $C^{18}O–C_2D_4$) ices…S32

Figure S25. PI-ReTOF-MS ion signal for $C_3H_nO_2$ (n = 4, 6, 8) versus temperature subliming from carbon monoxide-acetylene ($CO–C_2H_2$; $C^{18}O–C_2D_2$) ices…S33

Figure S26. PI-ReTOF-MS ion signal for $C_4H_nO_2$ (n = 4, 6, 8, 10) versus temperature subliming from carbon monoxide-ethane ($CO–C_2H_6$; $C^{18}O–C_2H_6$) ices…S34

Figure S27. PI-ReTOF-MS ion signal for $C_4H_nO_2$ (n = 4, 6, 8, 10) versus temperature subliming from carbon monoxide-ethylene ($CO–C_2H_4$; $C^{18}O–C_2D_4$) ices…S35

Figure S28. PI-ReTOF-MS ion signal for $C_4H_nO_2$ (n = 4, 6, 8, 10) versus temperature subliming from carbon monoxide-acetylene ($CO–C_2H_2$; $C^{18}O–C_2D_2$) ices…S36

Figure S29. PI-ReTOF-MS ion signal for $C_5H_nO_2$ (n = 6, 8) versus temperature subliming from carbon monoxide-ethane ($CO–C_2H_6$; $C^{18}O–C_2H_6$) ices…S37

Figure S30. PI-ReTOF-MS ion signal for $C_5H_nO_2$ (n = 6, 8) versus temperature subliming from carbon monoxide-ethylene ($CO–C_2H_4$; $C^{18}O–C_2D_4$) ices…S38

Figure S31. PI-ReTOF-MS ion signal for $C_5H_nO_2$ (n = 6, 8) versus temperature subliming from carbon monoxide-acetylene ($CO–C_2H_2$; $C^{18}O–C_2D_2$) ices…S39

Figure S32. PI-ReTOF-MS ion signal for $C_6H_nO_2$ (n = 8, 10, 12) versus temperature subliming from carbon monoxide-ethane ($CO–C_2H_6$; $C^{18}O–C_2H_6$) ices…S40

Figure S33. PI-ReTOF-MS ion signal for $C_6H_nO_2$ (n = 8, 10, 12) versus temperature subliming from carbon monoxide-ethylene ($CO–C_2H_4$; $C^{18}O–C_2D_4$) ices…S41

Figure S34. PI-ReTOF-MS ion signal for $C_6H_nO_2$ (n = 8, 10, 12) versus temperature subliming from carbon monoxide-acetylene ($CO–C_2H_2$; $C^{18}O–C_2D_2$) ices…S42

Figure S35. PI-ReTOF-MS ion signal for $C_4H_nO_3$ (n = 4, 6, 8) versus temperature subliming from carbon monoxide-ethane ($CO–C_2H_6$; $C^{18}O–C_2H_6$) ices…S43

Figure S36. PI-ReTOF-MS ion signal for $C_4H_nO_3$ (n = 4, 6, 8) versus temperature subliming from carbon monoxide-ethylene ($CO–C_2H_4$; $C^{18}O–C_2D_4$) ices…S44

Figure S37. PI-ReTOF-MS ion signal for $C_4H_nO_3$ (n = 4, 6, 8) versus temperature subliming from carbon monoxide-acetylene ($CO–C_2H_2$; $C^{18}O–C_2D_2$) ices…S45

Figure S38. PI-ReTOF-MS ion signal for $C_5H_nO_3$ (n = 6, 8) versus temperature subliming from carbon monoxide-ethane ($CO–C_2H_6$; $C^{18}O–C_2H_6$) ices…S46

Figure S39. PI-ReTOF-MS ion signal for $C_5H_nO_3$ (n = 6, 8) versus temperature subliming from carbon monoxide-ethylene ($CO–C_2H_4$; $C^{18}O–C_2D_4$) ices…S47

Figure S40. PI-ReTOF-MS ion signal for $C_5H_nO_3$ (n = 6, 8) versus temperature subliming from carbon monoxide-acetylene ($CO–C_2H_2$; $C^{18}O–C_2D_2$) ices…S48

References…S49

Table S1 Infrared absorption features recorded before and after the irradiation of each isotopic ice mixture at 5 K										
^{13}CO–$^{13}CD_4$		$C^{18}O$–C_2H_6		$C^{18}O$–C_2D_4		$C^{18}O$–C_2D_2				
Before Irradiation (cm^{-1})	After Irradiation (cm^{-1})	Before Irradiation (cm^{-1})	After Irradiation (cm^{-1})	Before Irradiation (cm^{-1})	After Irradiation (cm^{-1})	Before Irradiation (cm^{-1})	After Irradiation (cm^{-1})	Assignment	Carrier	Ref.
						5015		$\nu_1 + \nu_3$ (C_2D_2)	Combinations	1
			4610, 4461, 4441, 4409, 3844, 3378, 3329, 3306, 3186					$\nu_9 + 2\nu_6$, $\nu_9 + \nu_2$, $\nu_{11} + \nu_2$, $\nu_5 + \nu_{12}$, $\nu_9 + \nu_3$, $\nu_9 + \nu_6$, $\nu_{11} + \nu_3$, $\nu_{11} + \nu_6$ (C_2D_4)	Overtones/ Combinations	2-4
		4400, 4357, 4321, 4272, 4251, 4177, 4161, 4126, 4100, 4070						$\nu_8 + \nu_{10}$, $\nu_2 + \nu_7$, $\nu_6 + \nu_{10}$, $\nu_1 + \nu_6$, $\nu_2 + \nu_5$, $\nu_7 + \nu_{12}$, $\nu_7 + \nu_{12}$, $\nu_8 + \nu_{11} + \nu_{12}$, $\nu_8 + \nu_{11} + \nu_{12}$, $\nu_5 + \nu_{12}$ (C_2H_6)	Overtones/ Combinations	5
4154								$2\nu_1$ (^{13}CO)	Overtone	2, 6
		4147		4147		4154		$2\nu_1$ ($C^{18}O$)	Overtone	7, 8
						3294		$\nu_1 + \nu_5$ (C_2D_2)	Combinations	9
		3258						$\nu_4 + \nu_7$ (C_2H_6)	Combination	5
						3231		ν_3 (C_2H_2)	CH stretch	1
3216								$\nu_3 + \nu_4$ ($^{13}CD_4$)	Combinations	10-12
3078								$\nu_1 + \nu_4$ ($^{13}CD_4$)	Combinations	10-12
			3105					ν_{10} (C_2H_5)	CH2 asymmetric stretch	5, 7
			3091					ν_9 (C_2H_4)	CH_2 asymmetric stretch	4
			3008					ν_3 (CH_4)	degenerate stretch	13
		2973						ν_{10} (C_2H_6)	CH_3 degenerate stretch	5
		2959						ν_1 (C_2H_6)	CH_3 symmetric stretch	5
		2942						$\nu_8 + \nu_{11}$ (C_2H_6)	Combination	5
						2929		$\nu_3 + \nu_4$ (C_2D_2)	Combination	9
		2913						$\nu_8 + \nu_{11}$ (C_2H_6)	Combination	5
		2881						ν_5 (C_2H_6)	CH_3 symmetric stretch	5
		2852						$\nu_2 + \nu_4 + \nu_{12}$ (C_2H_6)	Combination	5

		2827						$\nu_6 + \nu_{11}$ (C_2H_6)	Combination	5
		2739						$\nu_2 + \nu_6$(C_2H_6)	Combination	5
						2680		ν_1 (C_2D_2)	CD stretch	9
		2648						$\nu_8 + \nu_{12}$ (C_2H_6)	Combination	5
					2590			ν_3 (C_2D_2)	CD stretch	8
							2585	ν_4 (C_4D_2)	CD stretch	14
							2573	ν_4 (C_4D_4)	CD stretch	15
		2558						$\nu_6 + \nu_9$ (C_2H_6)	Combination	5
						2555		ν_3 (C_2DH)	CD stretch	9
					2406	2408		ν_3 (C_2D_2)	CD stretch	4
		2359						$\nu_3 + \nu_6$ (C_2H_6)	Combination	5
						2341		ν_3 ($^{13}C_2D_2$)	CD stretch	9
			2338					ν_3 (^{18}OCO)	CO asymmetric stretch	7, 8
				2332				ν_9 (C_2D_4)	CD_2 asymmetric stretch	4
						2325		$\nu_2 + \nu_5$ (C_2D_2)	Combination	9
			2323					ν_3 (CO_2)	CO asymmetric stretch	7, 8
			2310		2307			ν_3 ($C^{18}O_2$)	CO asymmetric stretch	7, 8
	2276							ν_6 ($^{13}CO_2$)	CO asymmetric stretch	2, 16
2259								ν_3 (CD_4)	degenerate stretch	10-12, 17
2237								ν_3 ($^{13}CD_4$)	degenerate stretch	10-12, 17
							2232	ν_{10} (C_2D_6)/ ν_{11} (C_2D_4)	CD_3 degenerate stretch/ CH_2 symmetric stretch	4, 5
					2228			ν_7 (C_2D_6)	CD_3 degenerate stretch	5
			2227					ν_3 ($C_3{}^{18}O_2$)	CO asymmetric stretch	7, 8
					2219			$\nu_2 + \nu_8$ (C_2D_6)	Combination	5
	2214							ν_{10} ($^{13}C_2D_6$)	degenerate stretch	18, 19
	2203							$\nu_2 + \nu_8$ ($^{13}C_2D_6$)	Combination	20

				2192				ν_{11} (C_2D_4)	CD_2 symmetric stretch	4
			2161					ν_1 ($C_3{}^{18}O_2$)	CO stretch	7, 8
	2185							ν_1 ($^{13}C_2D_6$)	CD_3 symmetric stretch	5
	2177							ν_{11} ($^{13}C_2D_4$)	CD_2 symmetric stretch	21
2137		2136		2137		2139		ν_1 (CO)	CO stretch	6-8
2090								ν_1 (^{13}CO)	CO stretch	6-8
		2089		2084		2088		ν_1 ($C^{18}O$)	CO stretch	6-8
	2073							ν_5 (C_2D_6)	CD_3 symmetric stretch	19
2063								$\nu_2 + \nu_4$ (CD_4)	Combination	12
	2055							ν_5 ($^{13}C_2D_6$)	CD_3 symmetric stretch	19
2038								$\nu_2 + \nu_4$ ($^{13}CD_4$)	Combination	12
	2026							$\nu_6 + \nu_9$ ($^{13}C_2D_6$)	Combination	5, 18, 22
1962								$2\nu_4$ ($^{13}CD_4$)	Overtone	12
			1811					ν_3 ($HC^{18}O$)	CO stretch	6-8
							1800	[a]	CO stretch	6-8, 23
	1774							ν_3 ($D^{13}CO$)	CO stretch	6-8, 23
					1772		1773	ν_3 ($DC^{18}O$)	CO stretch	6-8 16
					1768			ν_2 ($DOC^{18}O$)	CO stretch	8
	1690–1660		1740-1600		1680-1640		1700-1670	[a]	CO stretch	23
		1463						ν_{11} (C_2H_6)	CH_3 deformation	5
			1435					ν_{12} (C_2H_4)	CH_2 scissor	4
		1371						ν_6 (C_2H_6)	CH_3 symmetric deformation	5
			1301					ν_4 (CH_4)	Degenerate stretch	13
						1085		$\nu_4 + \nu_5$ (C_2D_2)	Combination	9
			1083					ν_2 ($HC^{18}O$)	CO stretch	6-8, 23
				1073				ν_{12} (C_2D_4)	CD_2 scissor	4
	1067							ν_{12} ($^{13}C_2D_4$)	CD_2 symmetric stretch	21
985								ν_4 ($^{13}CD_4$)	Degenerate stretch	10-12,

										17
			951					ν_7 (C_2H_4)	CH_2 wag	4
		820						ν_{12} (C_2H_6)	Bending	5
			758					ν_5 (C_2H_2)	CCH bend	1
				723				ν_7 (C_2D_4)	CD_2 wag	4
						707		ν_5 (C_2D_2)	CH bend	9
						565		ν_4 (C_2D_2)	CD bend	9

[a] Carbonyl stretching region (saturated/unsaturated aldehydes/ketones with mono-/di-/tri-/tetra- substituted side chains)

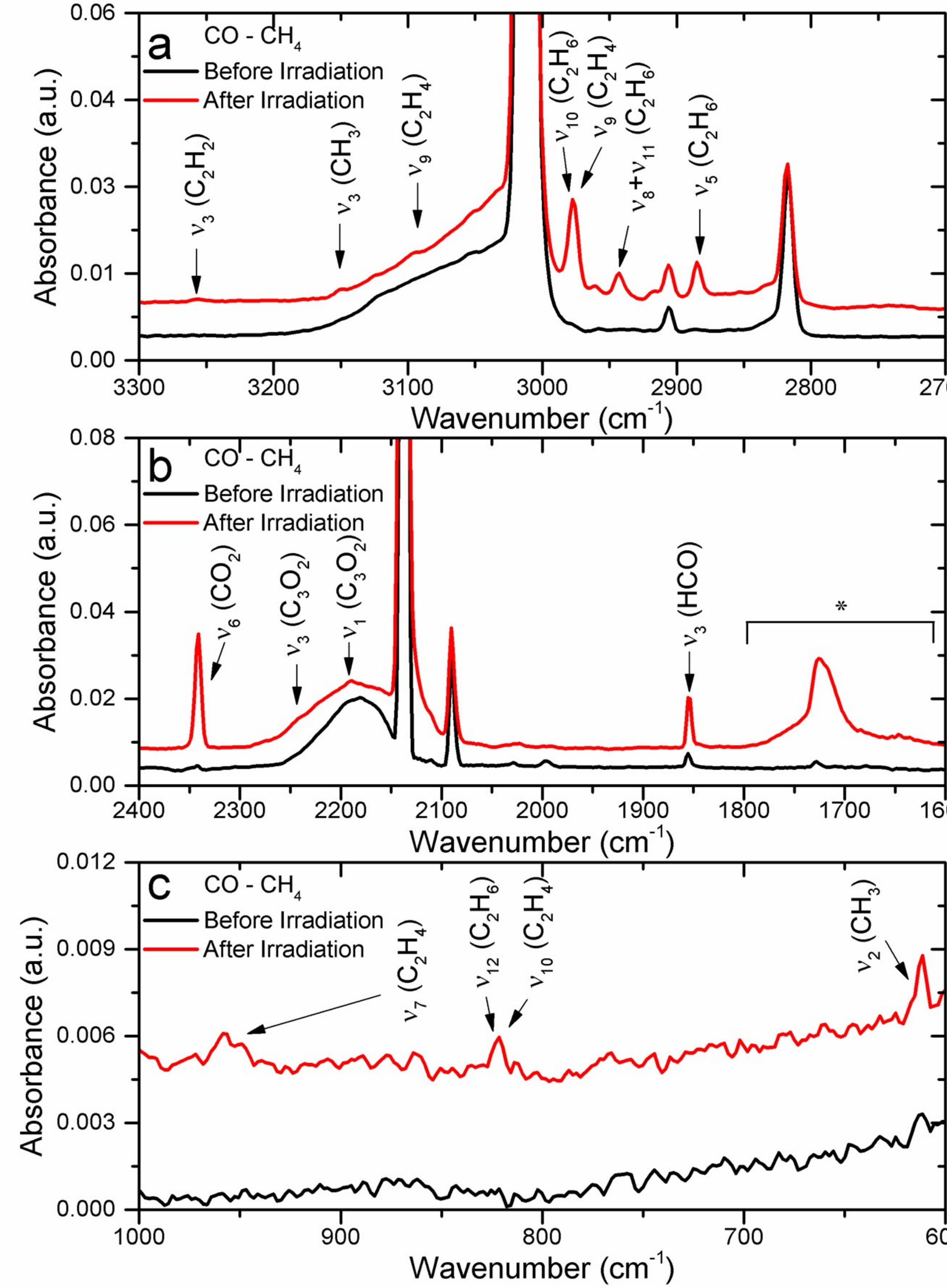

Fig. S1 Infrared spectra before (black) and after (red) irradiation of carbon monoxide-methane ($CO–CH_4$) ice from (a) 2700-3300 cm^{-1}, (b) 1600-2400 cm^{-1}, and (c) 600-1000 cm^{-1}. Assignments of reactants and products are compiled in Table 2 and * corresponds to carbonyl containing species.

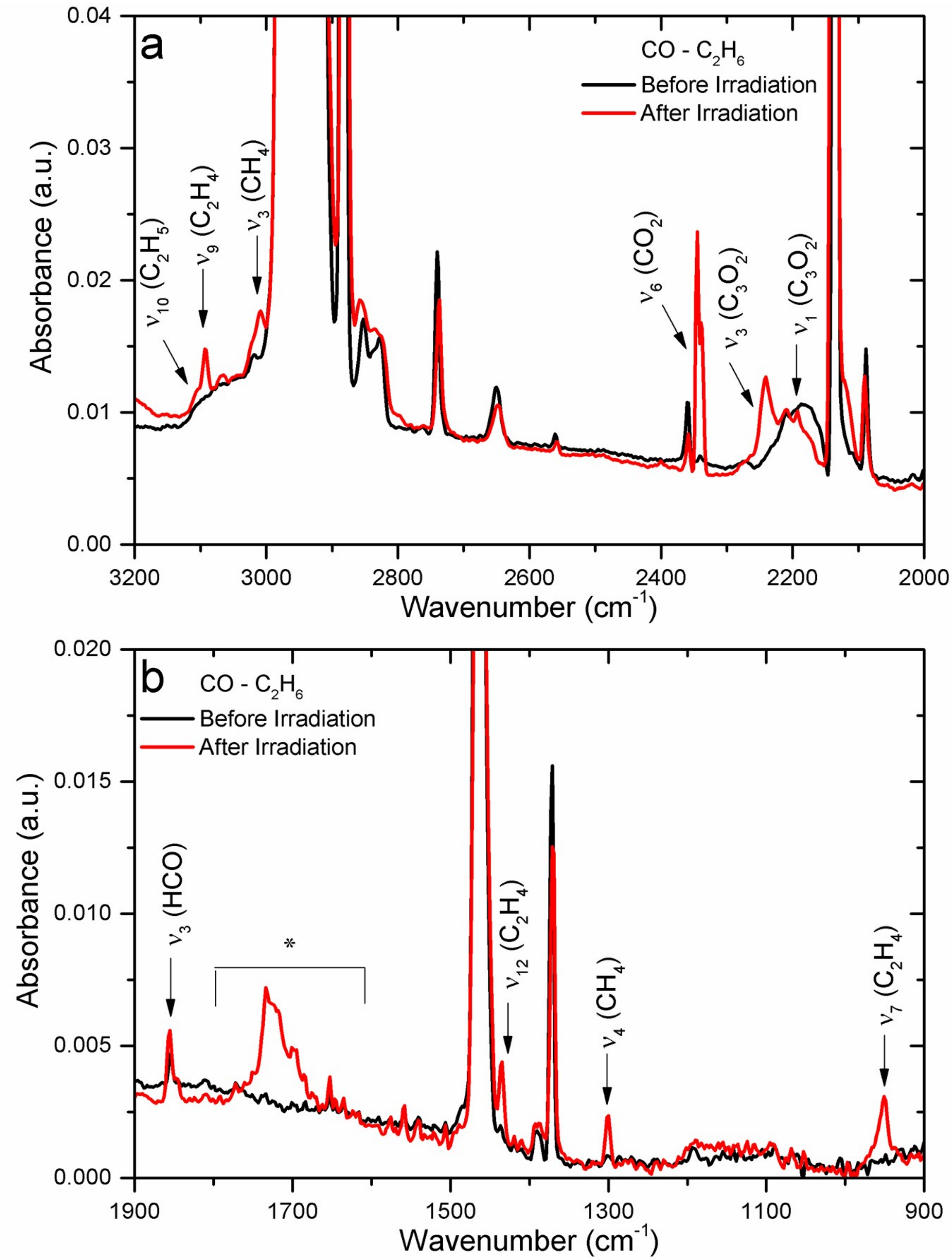

Fig. S2 Infrared spectra before (black) and after (red) irradiation of carbon monoxide-ethane ($CO–C_2H_6$) ice from (a) 2000-3200 cm^{-1} and (b) 900-1900 cm^{-1}. Assignments of reactants and products are compiled in Table 2 and * corresponds to carbonyl containing species.

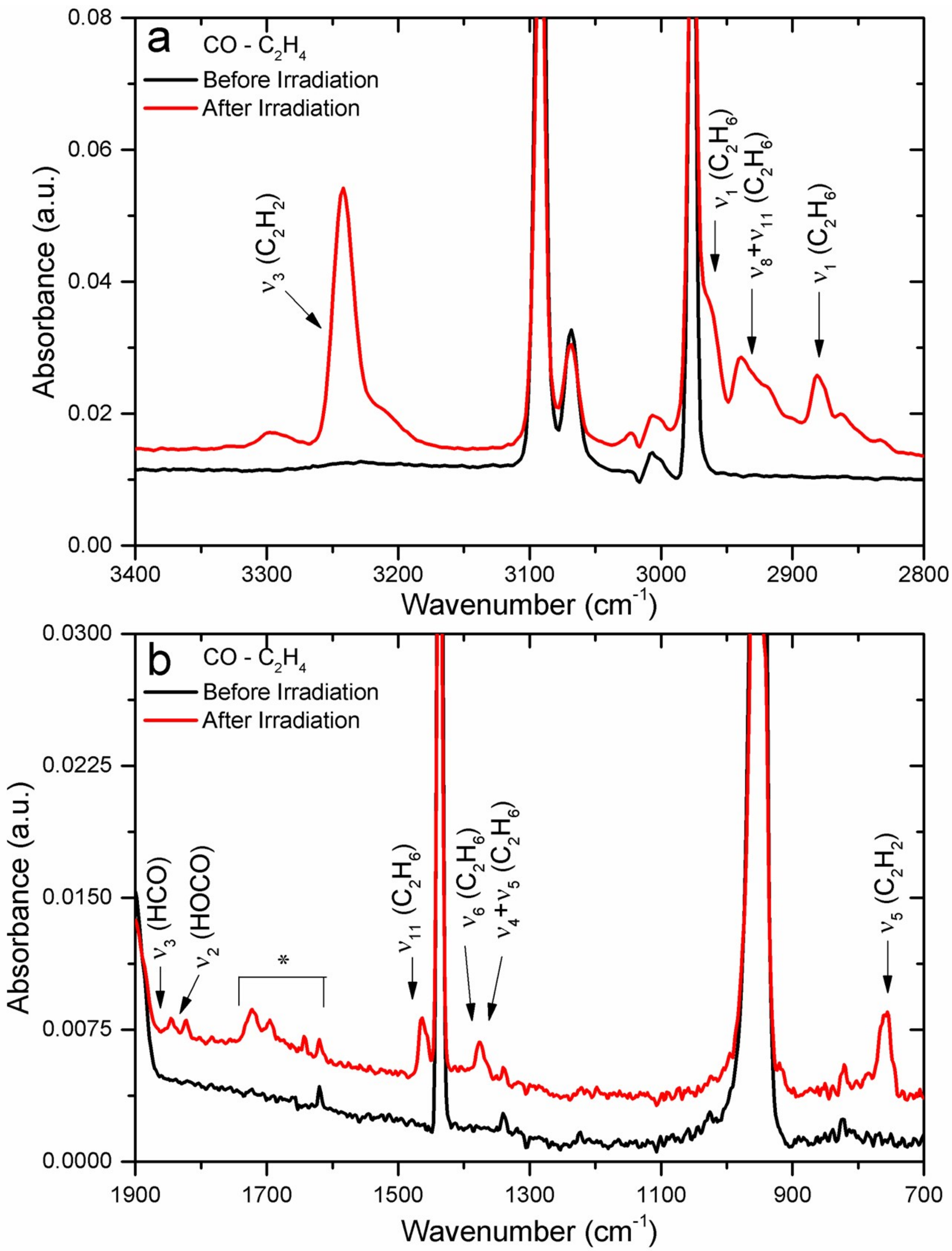

Fig. S3 Infrared spectra before (black) and after (red) irradiation of carbon monoxide-ethylene ($CO–C_2H_4$) ice from (a) 2800-3400 cm^{-1} and (b) 700-1900 cm^{-1}. Assignments of reactants and products are compiled in Table 2 and *corresponds to carbonyl containing species.

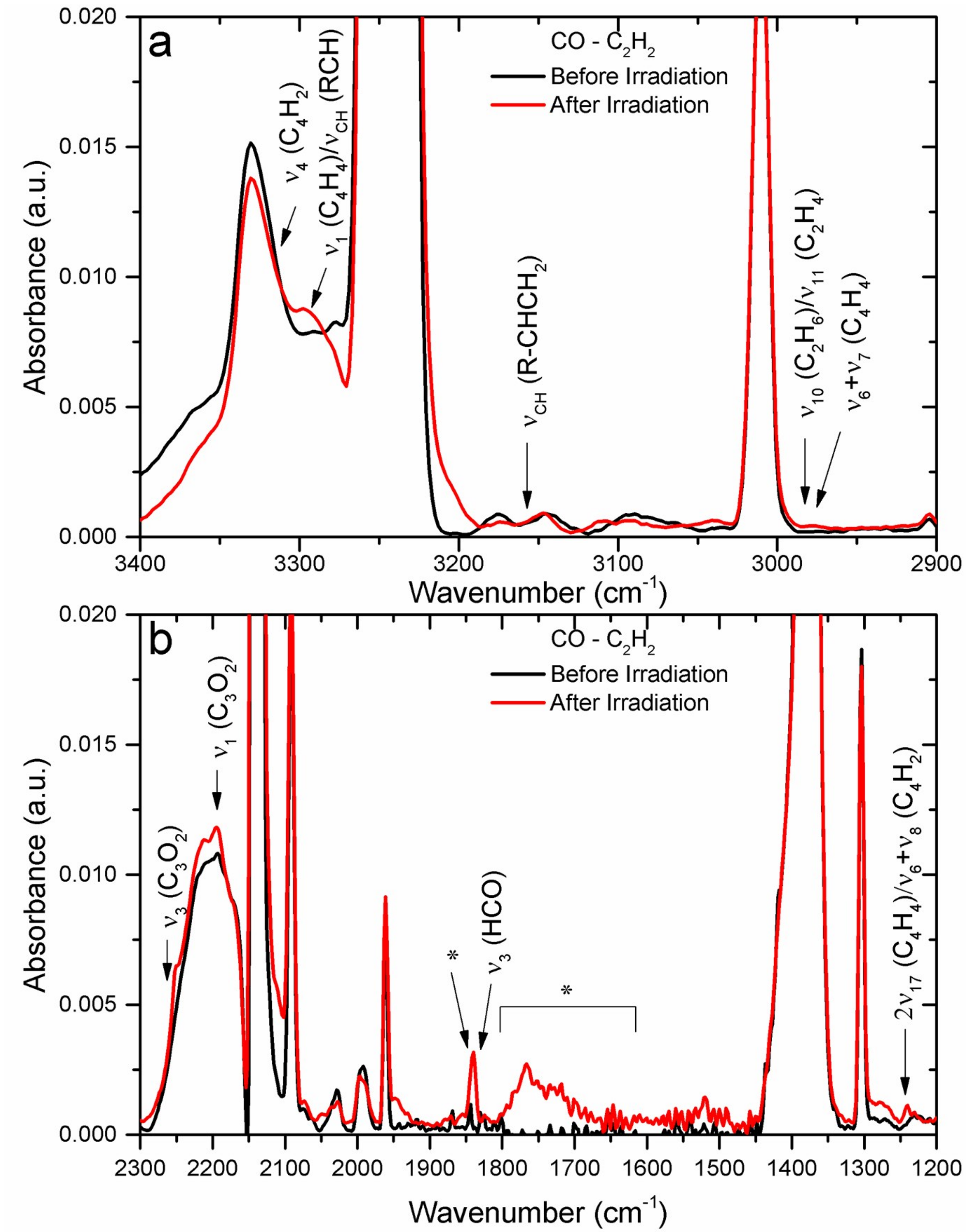

Fig. S4 Infrared spectra before (black) and after (red) irradiation of carbon monoxide-acetylene (CO–C_2H_2) ice from (a) 2900-3400 cm^{-1} and (b) 1200-2300 cm^{-1}. Assignments of reactants and products are compiled in Table 2 and *corresponds to carbonyl containing species.

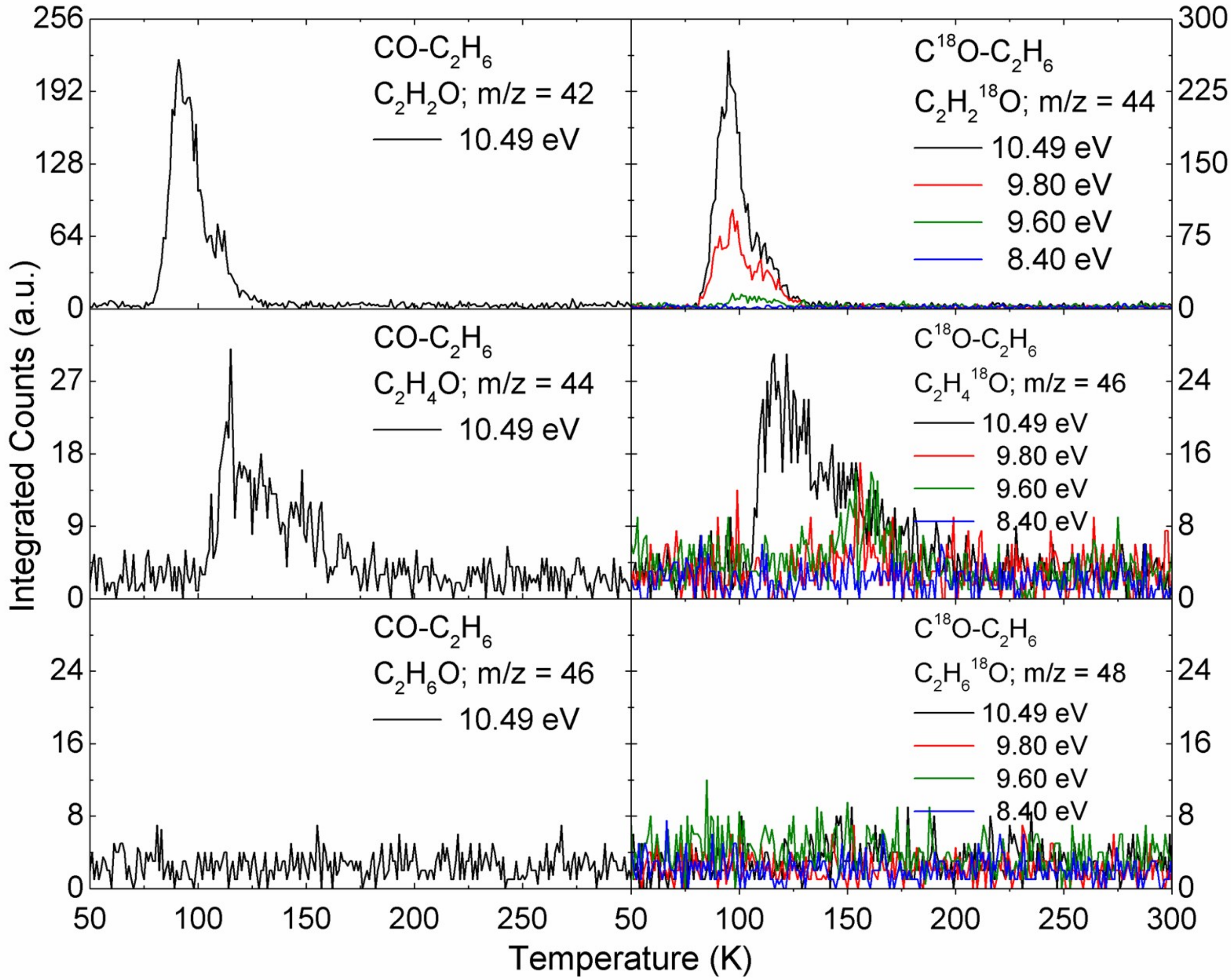

Fig. S5 PI-ReTOF-MS ion signal for C_2H_nO (n = 2, 4, 6) versus temperature subliming from carbon monoxide-ethane (CO–C_2H_6; $C^{18}O$–C_2H_6) ices

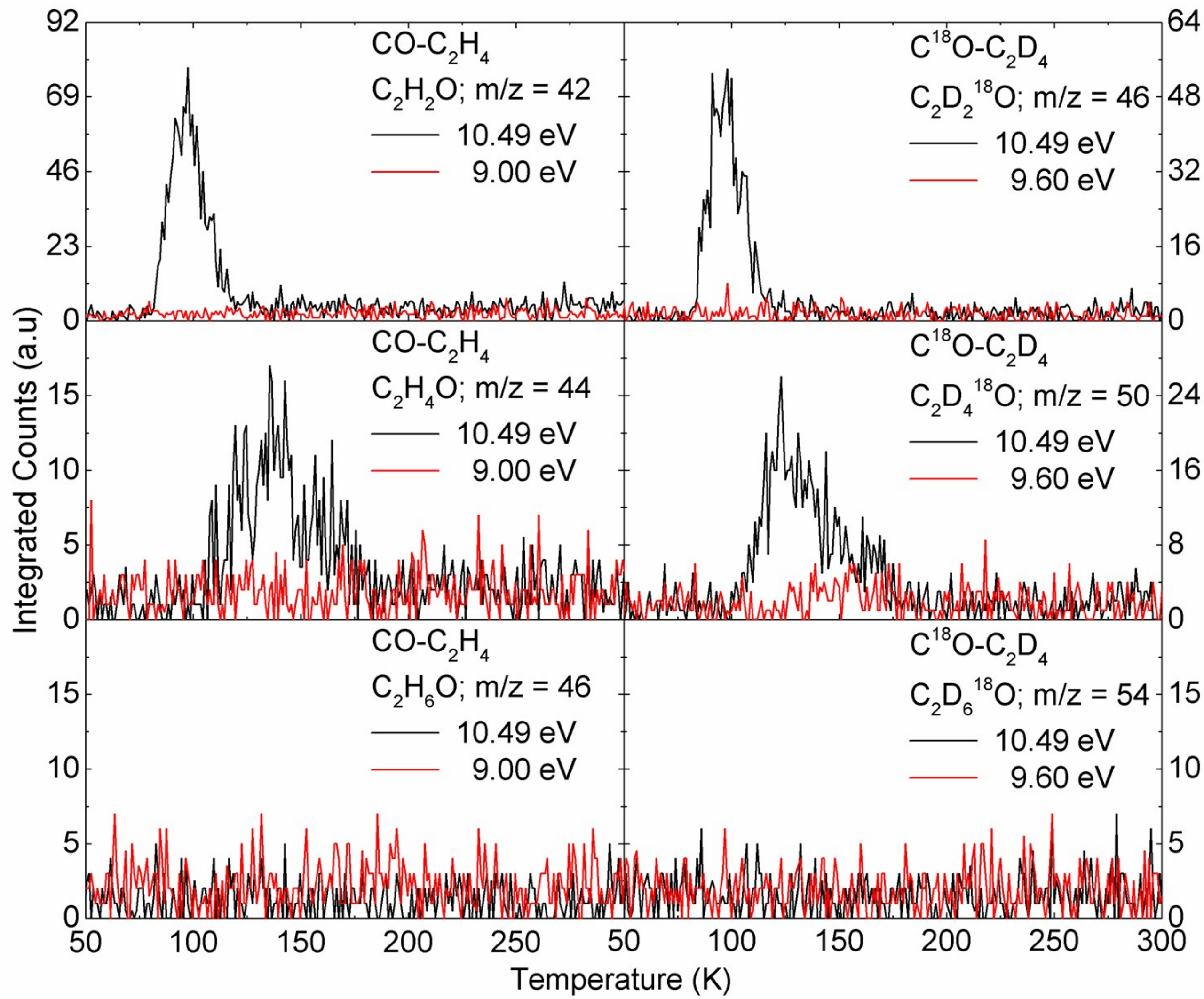

Fig. S6 PI-ReTOF-MS ion signal for C_2H_nO (n = 2, 4, 6) versus temperature subliming from carbon monoxide-ethylene ($CO–C_2H_4$; $C^{18}O–C_2D_4$) ices.

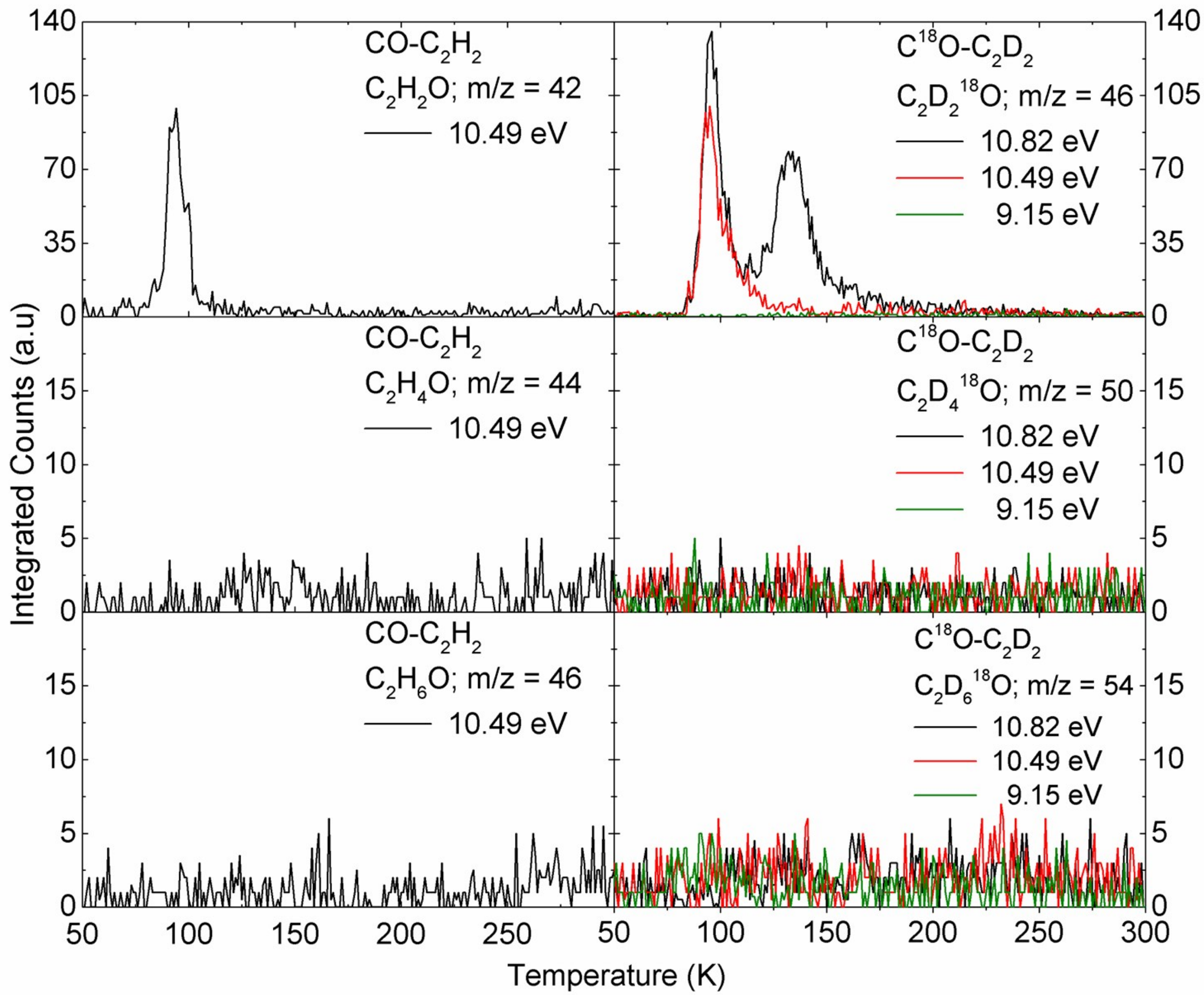

Fig. S7 PI-ReTOF-MS ion signal for C_2H_nO (n = 2, 4, 6) versus temperature subliming from carbon monoxide-acetylene (CO–C_2H_2; $C^{18}O$–C_2D_2) ices.

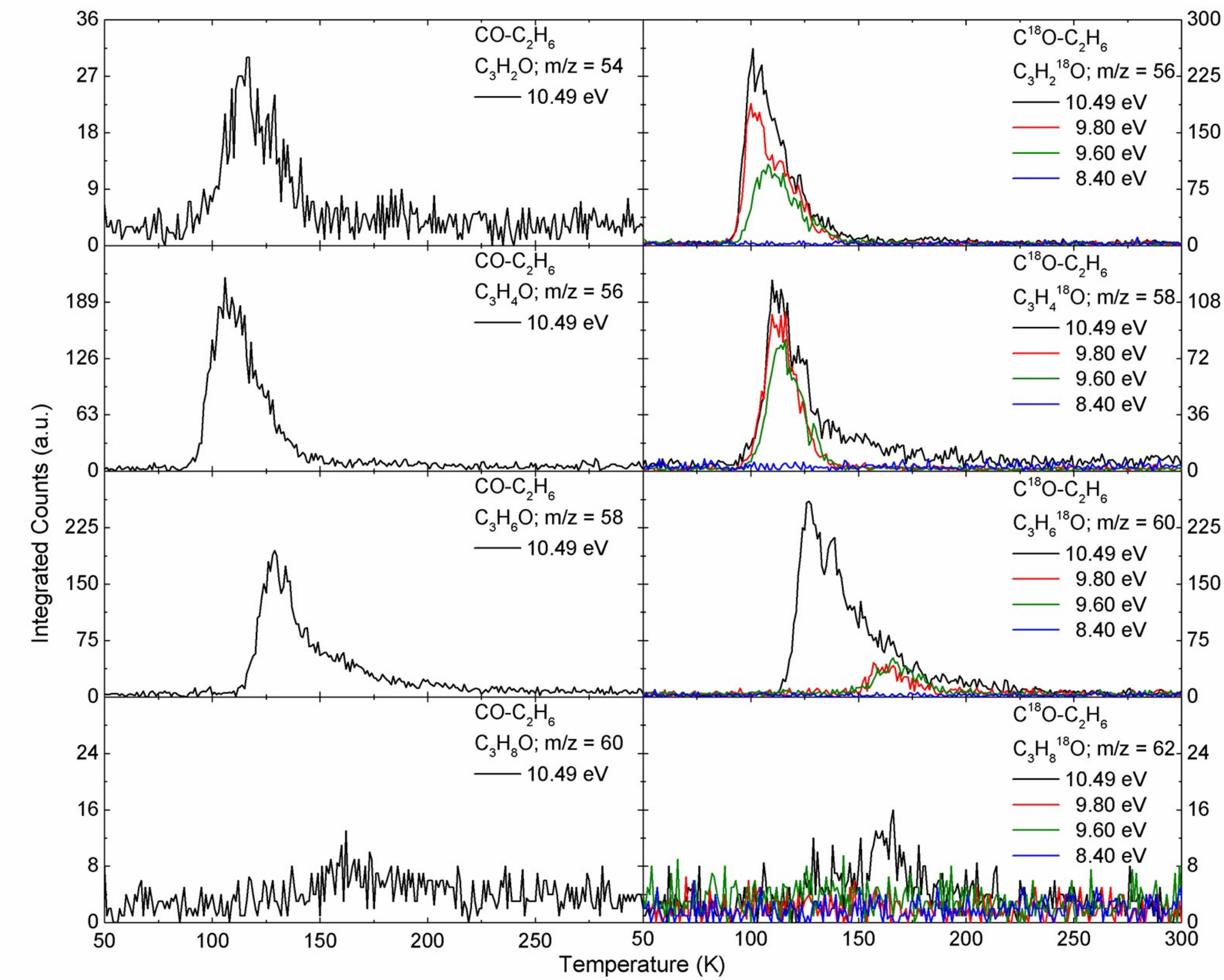

Fig. S8 PI-ReTOF-MS ion signal for C_3H_nO (n = 2, 4, 6, 8) versus temperature subliming from carbon monoxide-ethane (CO–C_2H_6; $C^{18}O$–C_2H_6) ices.

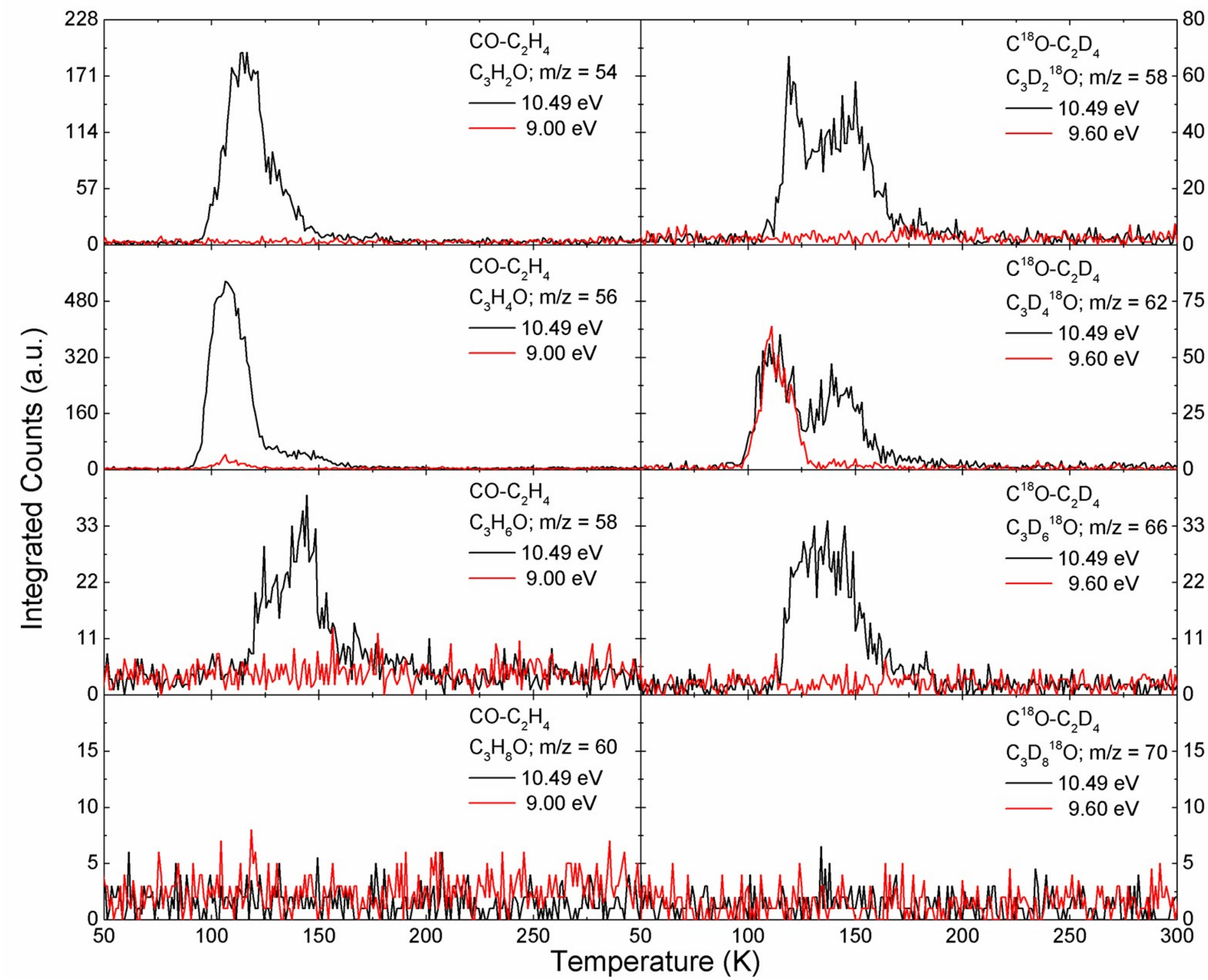

Fig. S9 PI-ReTOF-MS ion signal for C_3H_nO (n = 2, 4, 6, 8) versus temperature subliming from carbon monoxide-ethylene (CO–C_2H_4; $C^{18}O$–C_2D_4) ices.

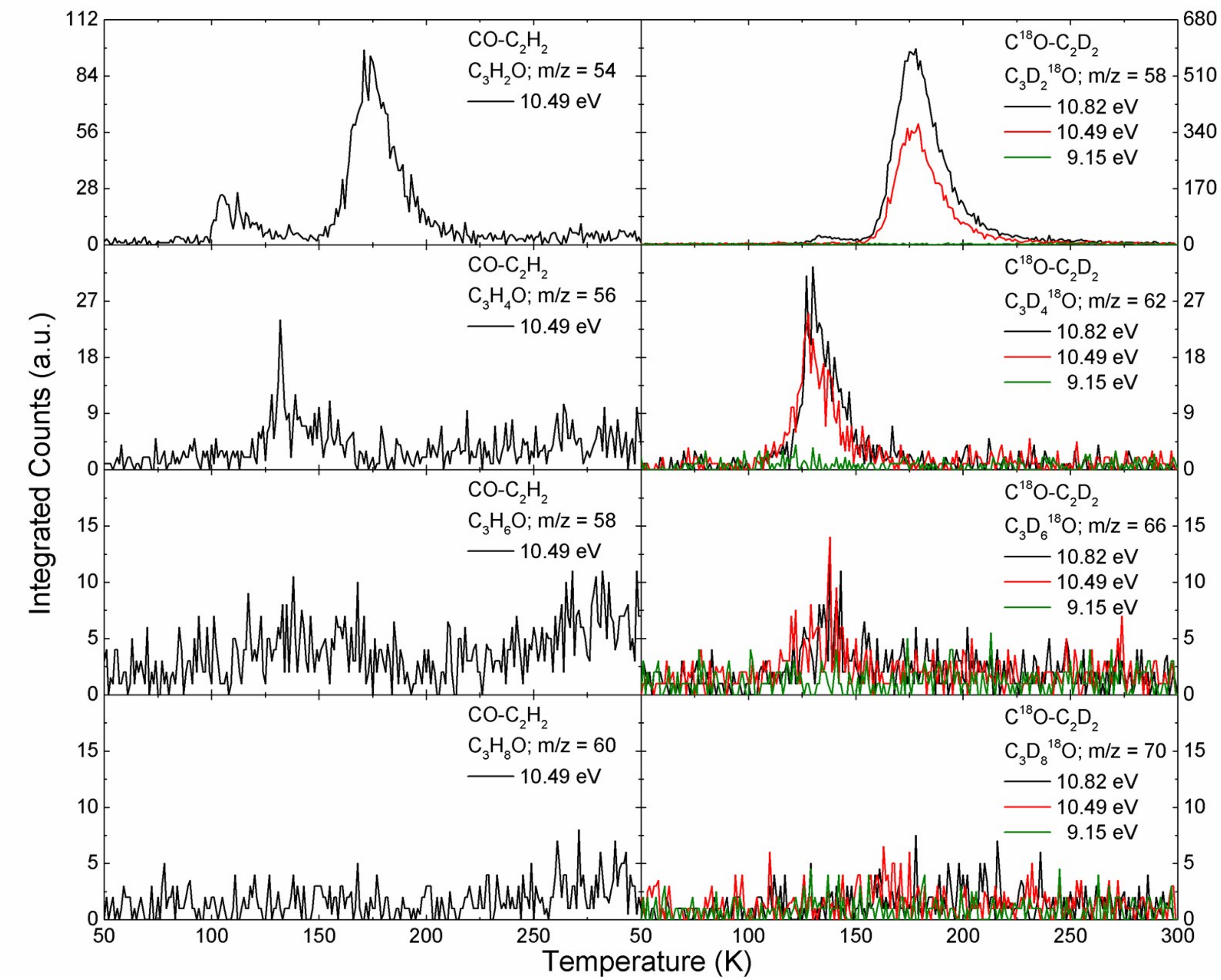

Fig. S10 PI-ReTOF-MS ion signal for C_3H_nO (n = 2, 4, 6, 8) versus temperature subliming from carbon monoxide-acetylene (CO–C_2H_2; $C^{18}O$–C_2D_2) ices.

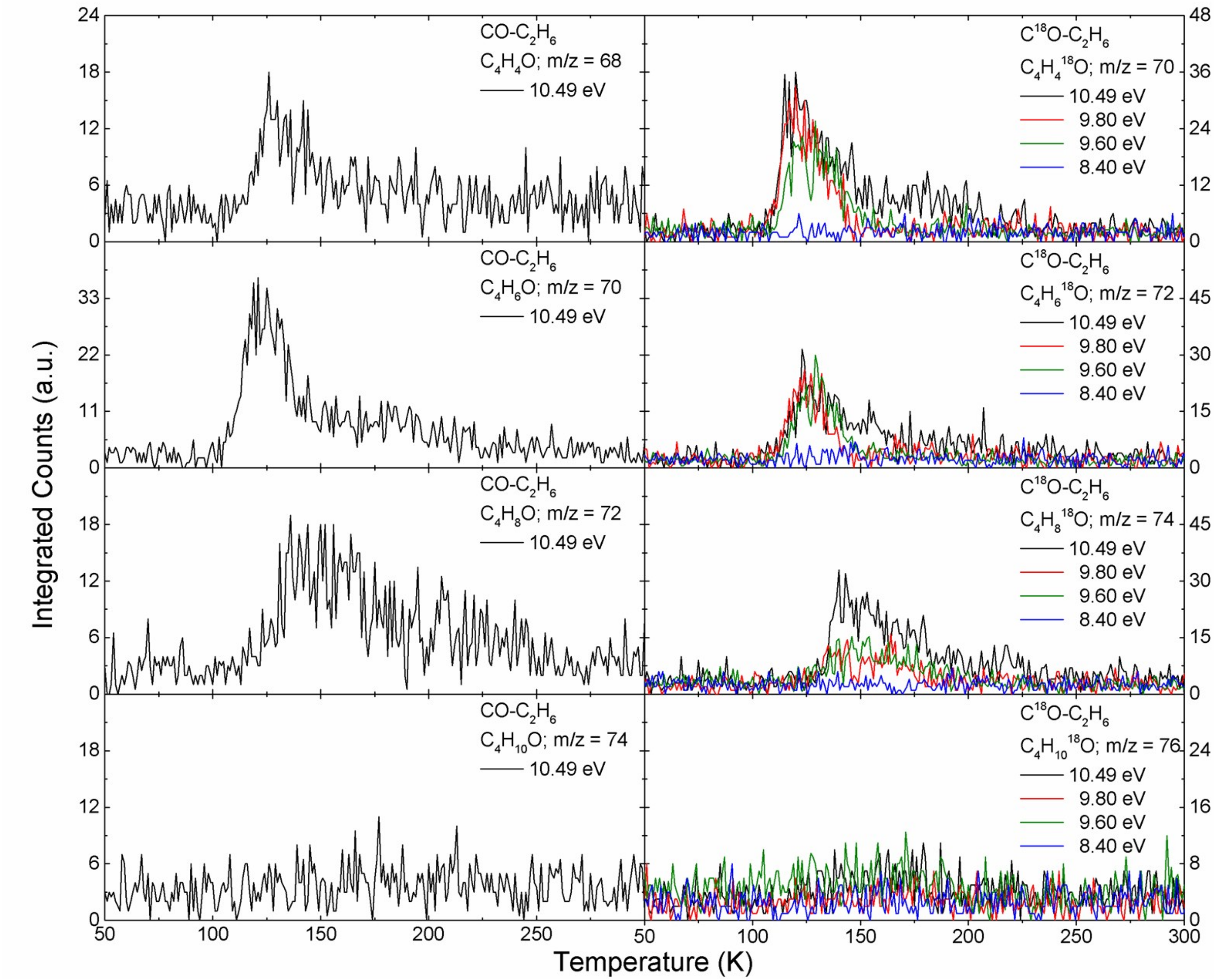

Fig. S11 PI-ReTOF-MS ion signal for C_4H_nO (n = 4, 6, 8, 10) versus temperature subliming from carbon monoxide-ethane (CO–C_2H_6; $C^{18}O$–C_2H_6) ices.

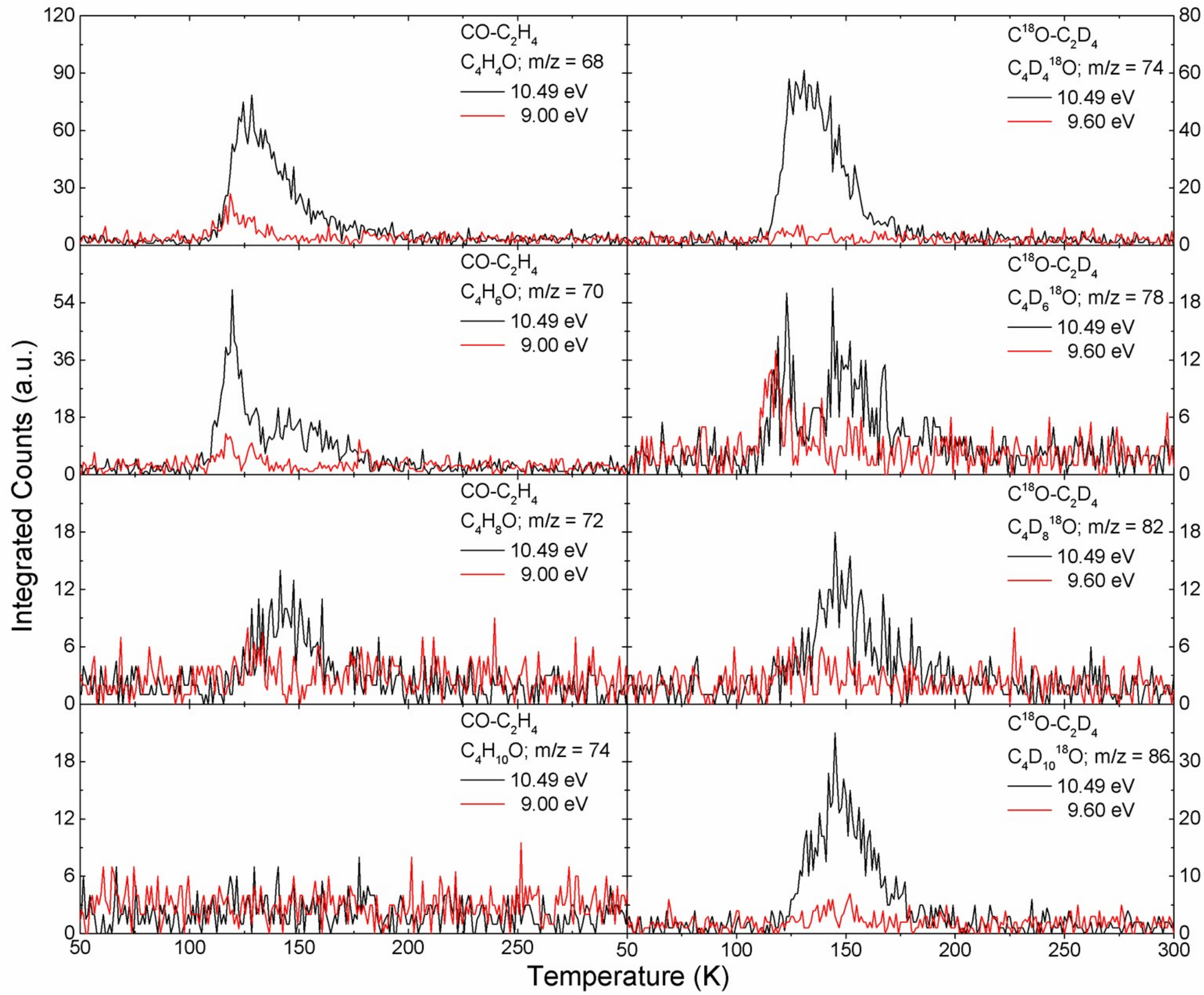

Fig. S12 PI-ReTOF-MS ion signal for C_4H_nO (n = 4, 6, 8, 10) versus temperature subliming from carbon monoxide-ethylene (CO–C_2H_4; $C^{18}O$–C_2D_4) ices.

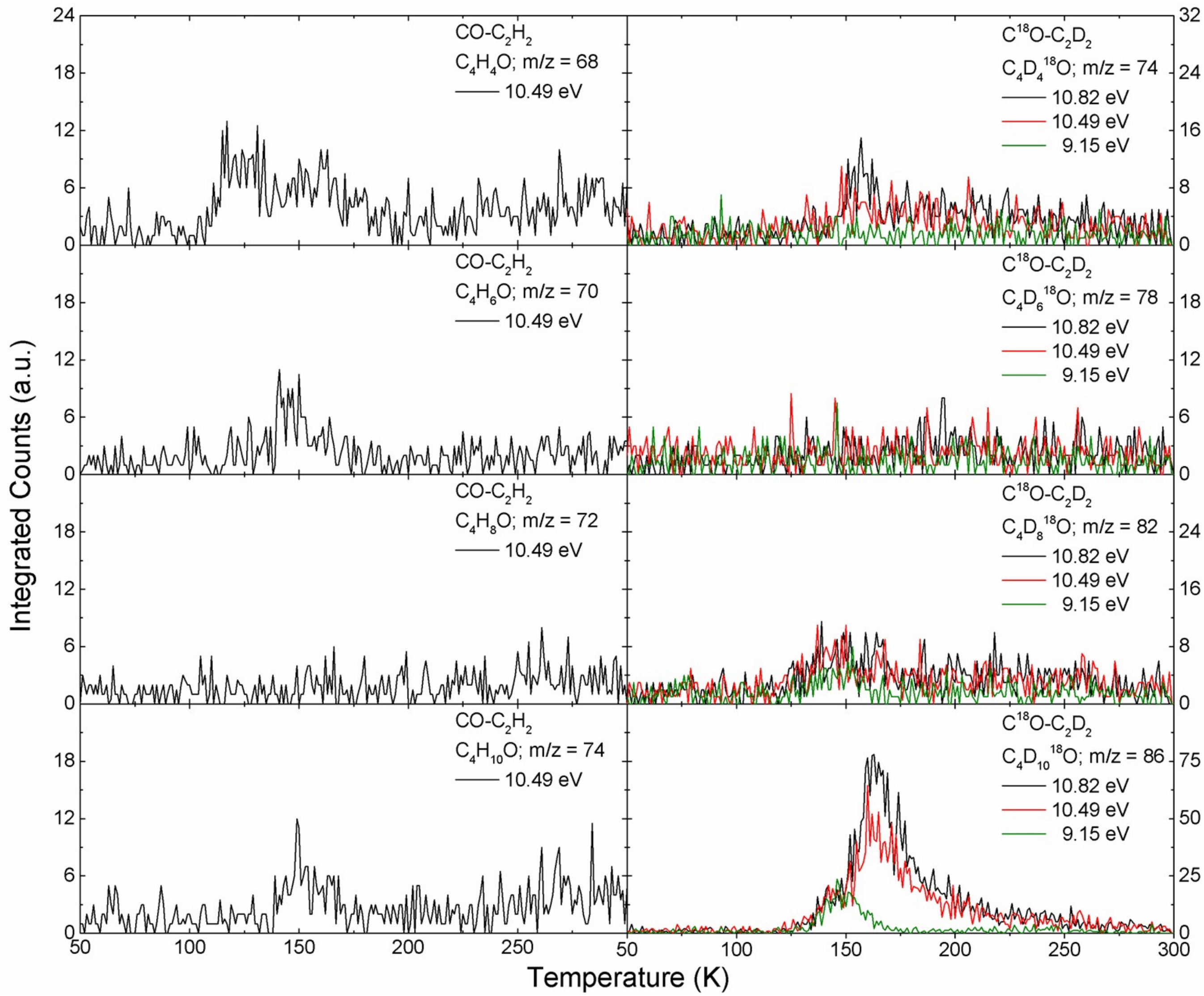

Fig. S13 PI-ReTOF-MS ion signal for C_4H_nO (n = 4, 6, 8, 10) versus temperature subliming from carbon monoxide-acetylene (CO–C_2H_2; $C^{18}O$–C_2D_2) ices.

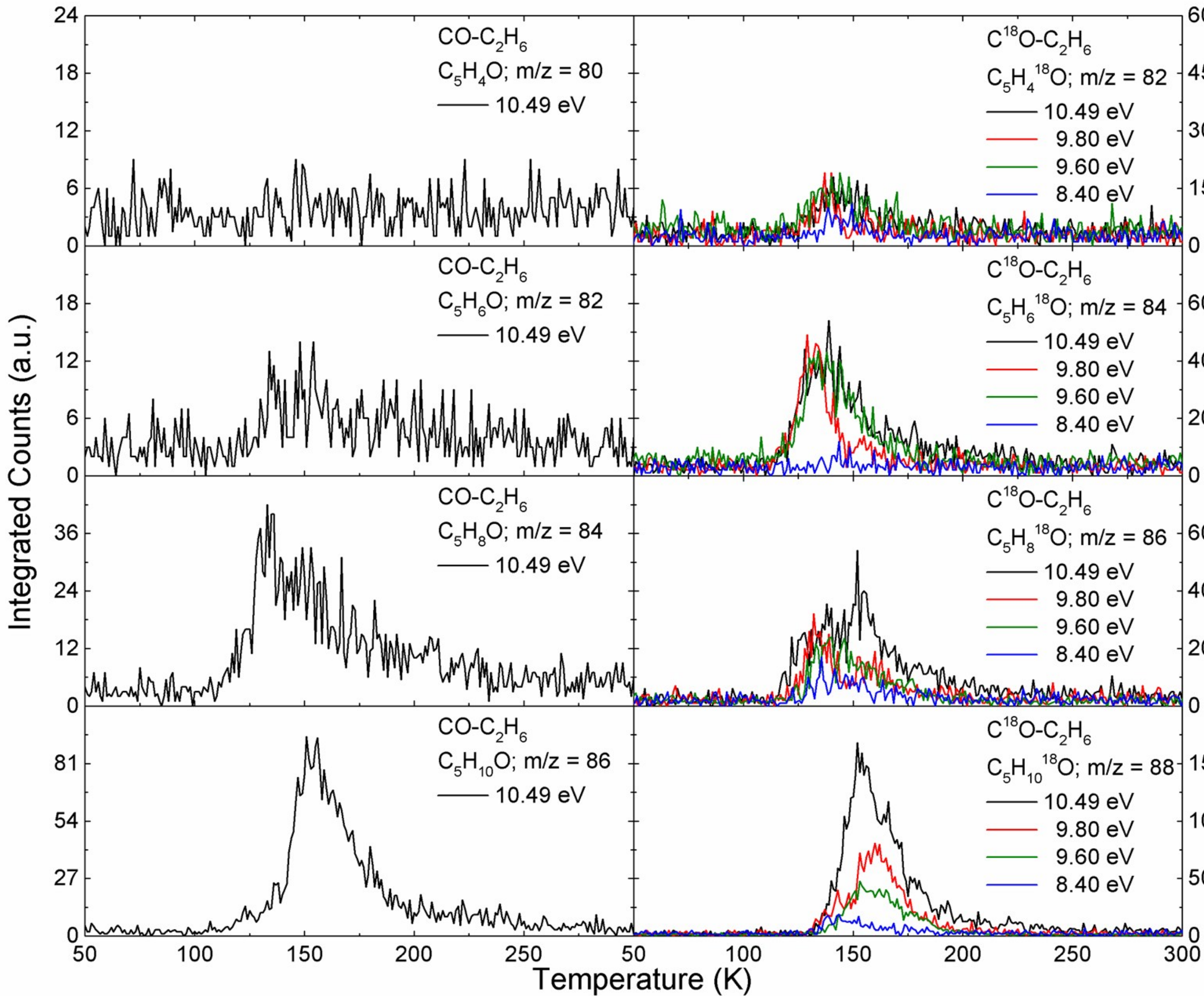

Fig. S14 PI-ReTOF-MS ion signal for C_5H_nO (n = 4, 6, 8, 10) versus temperature subliming from carbon monoxide-ethane (CO–C_2H_6; $C^{18}O$–C_2H_6) ices.

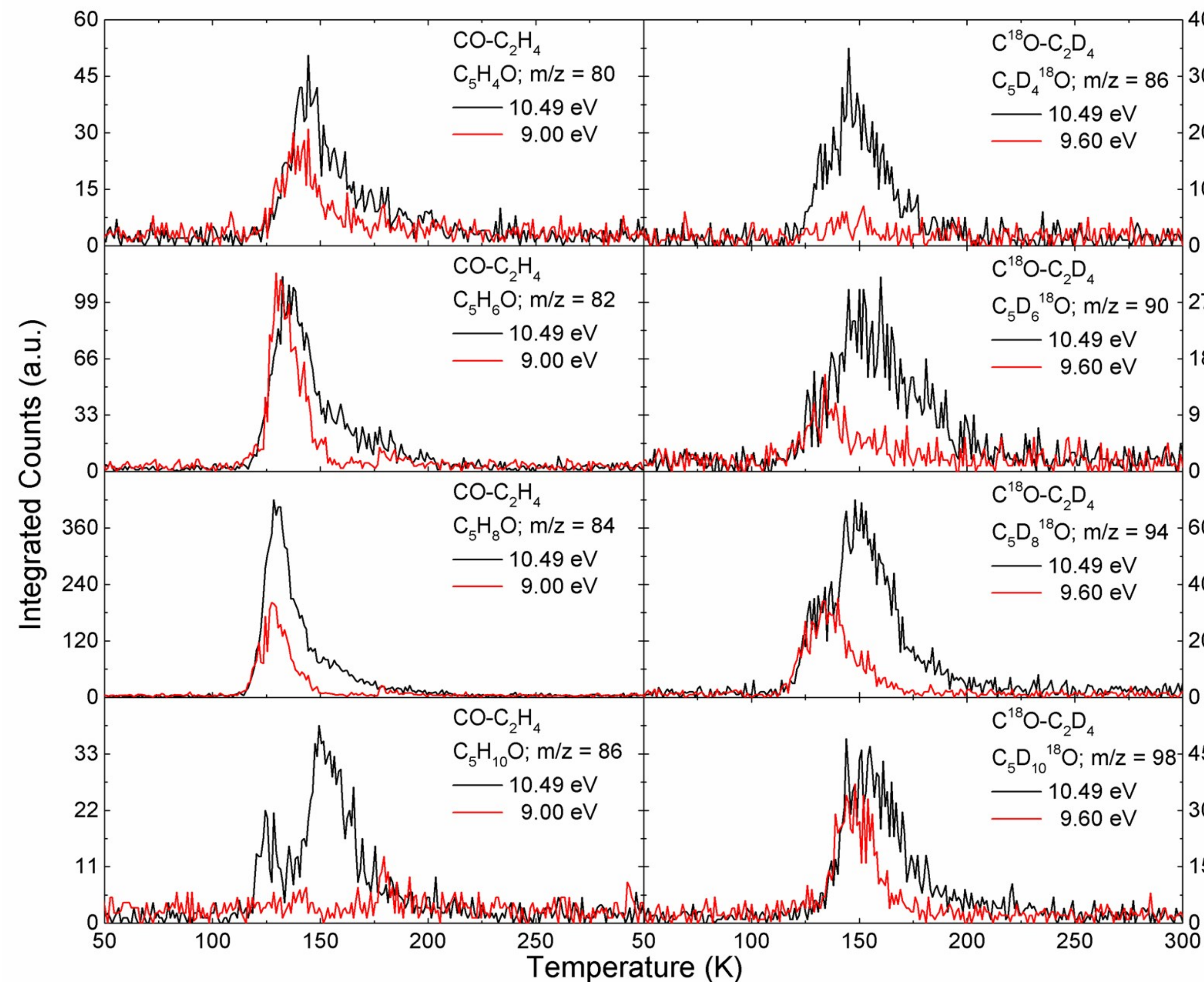

Fig. S15 PI-ReTOF-MS ion signal for C_5H_nO (n = 4, 6, 8, 10) versus temperature subliming from carbon monoxide-ethylene (CO–C_2H_4; $C^{18}O$–C_2D_4) ices.

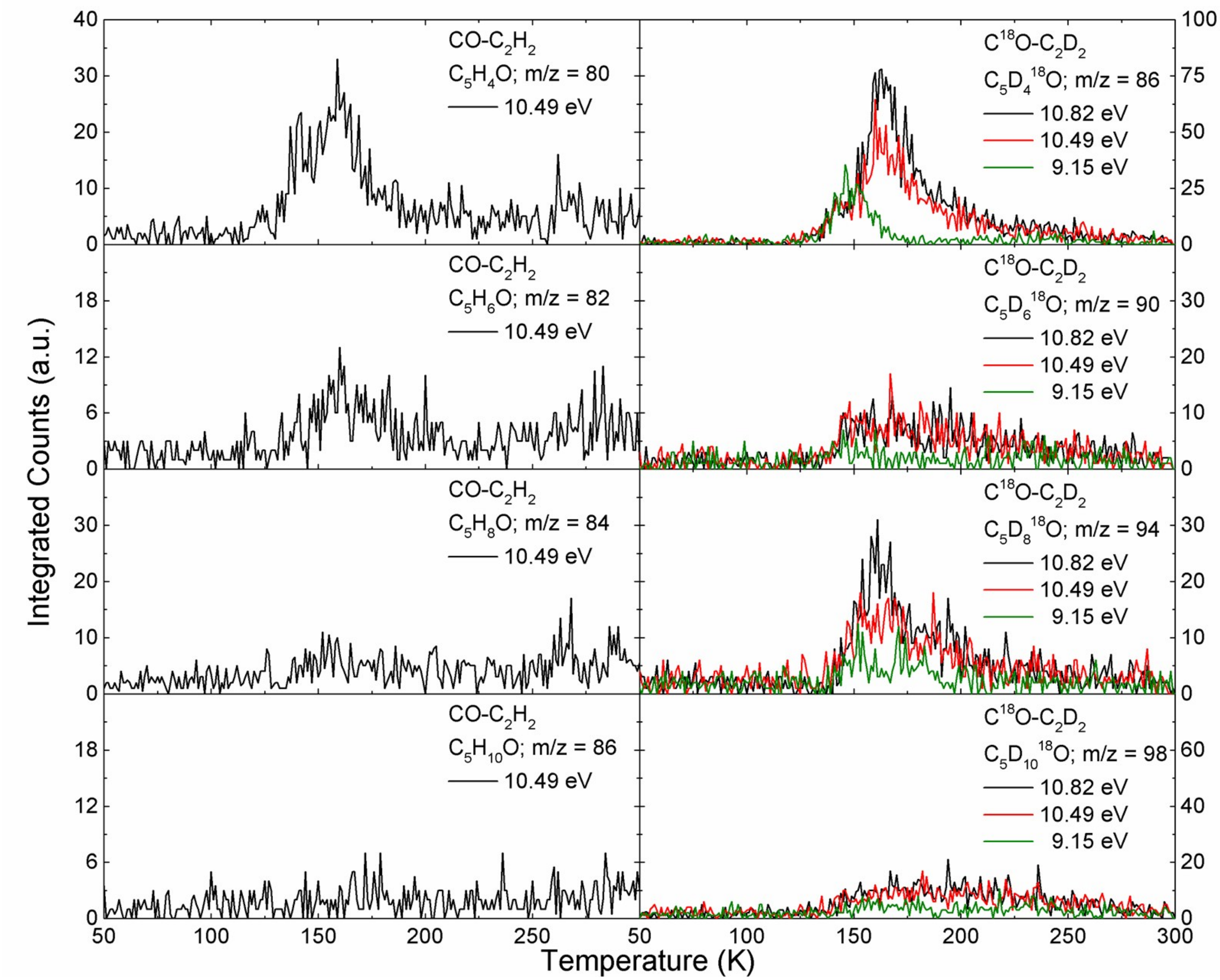

Fig. S16 PI-ReTOF-MS ion signal for C_5H_nO (n = 4, 6, 8, 10) versus temperature subliming from carbon monoxide-acetylene (CO–C_2H_2; $C^{18}O$–C_2D_2) ices.

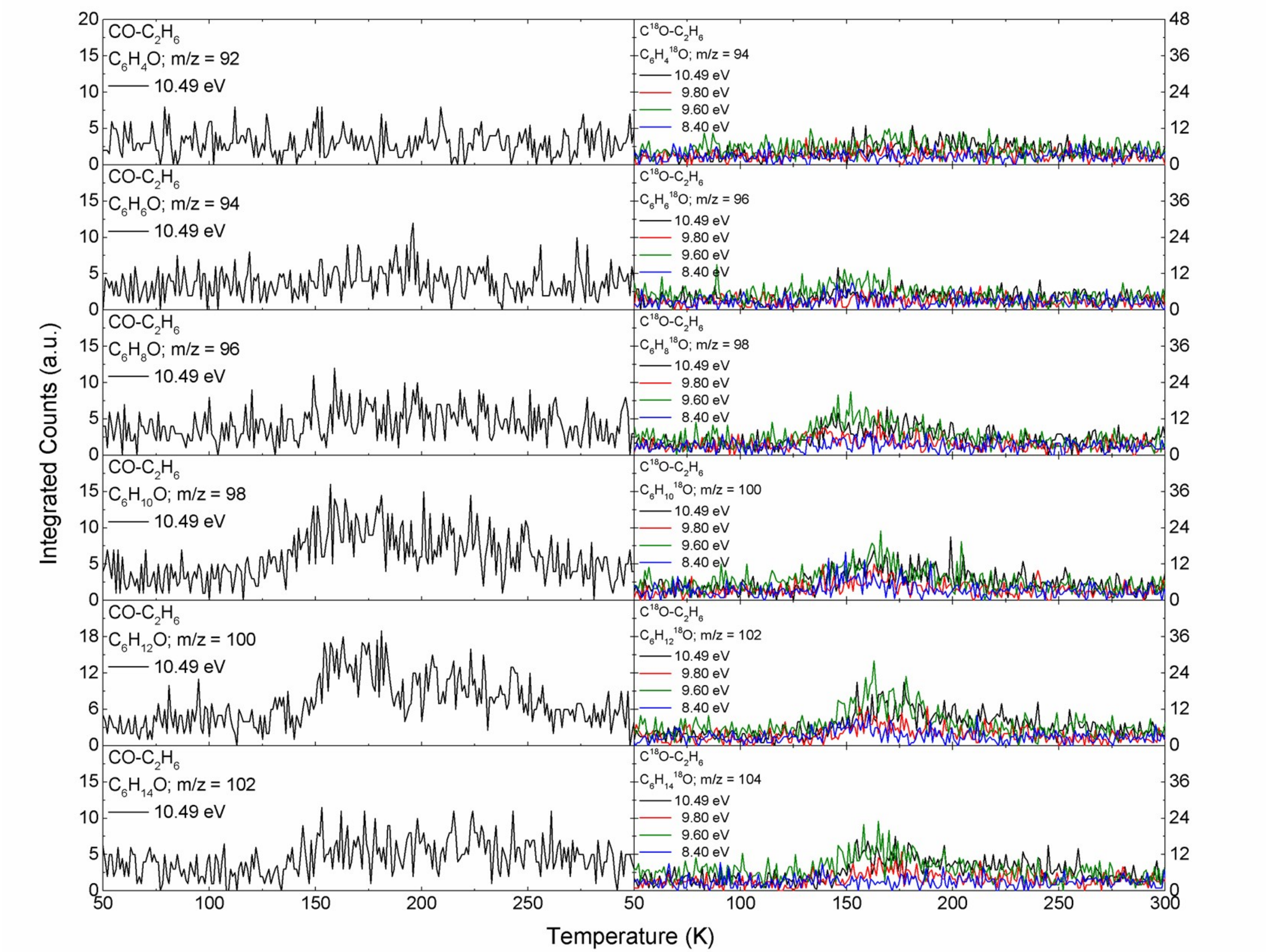

Fig. S17 PI-ReTOF-MS ion signal for C_6H_nO (n = 4, 6, 8, 10, 12, 14) versus temperature subliming from carbon monoxide-ethane ($CO–C_2H_6$; $C^{18}O–C_2H_6$) ices.

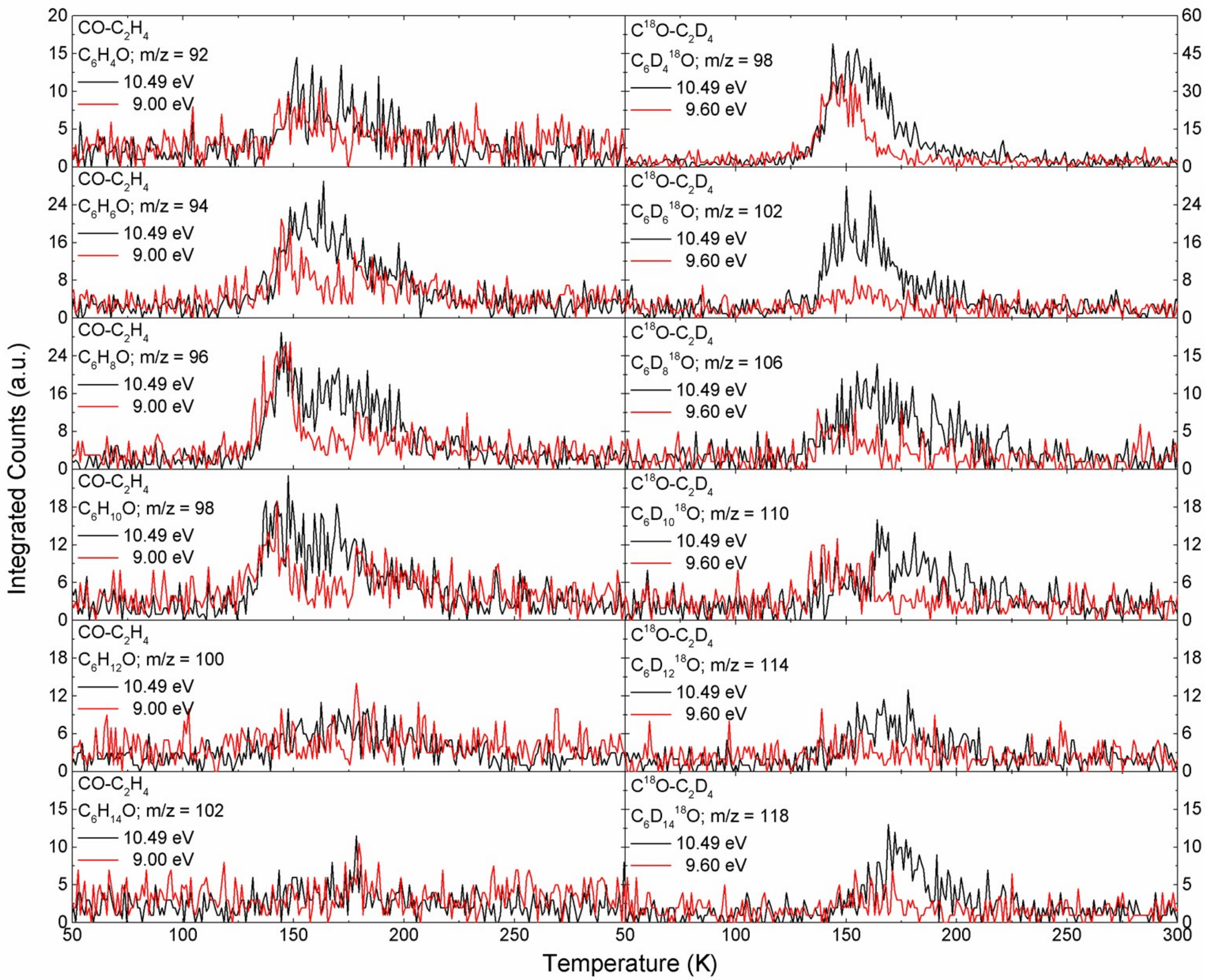

Fig. S18 PI-ReTOF-MS ion signal for C_6H_nO (n = 4, 6, 8, 10, 12, 14) versus temperature subliming from carbon monoxide-ethylene ($CO–C_2H_4$; $C^{18}O–C_2D_4$) ices.

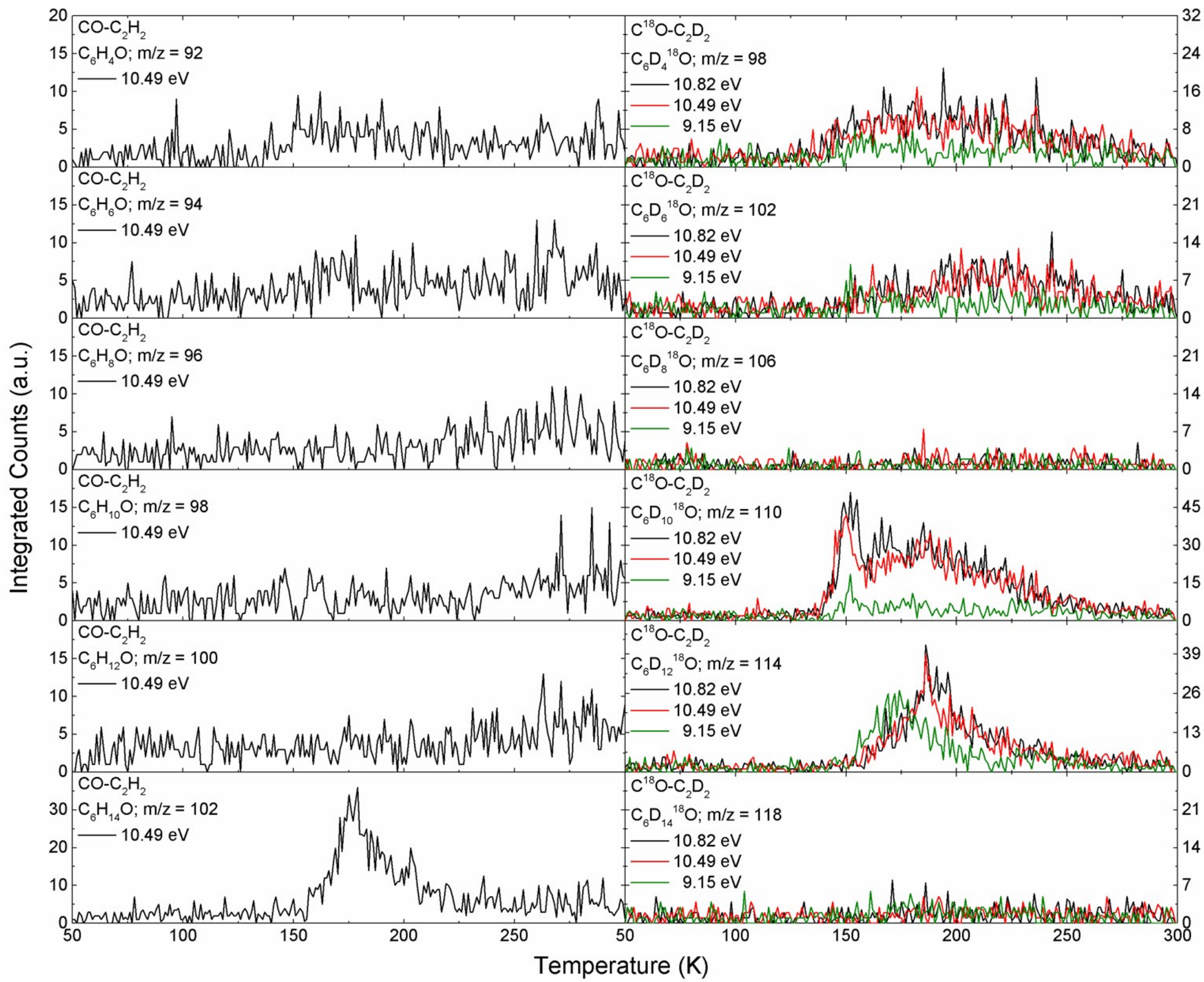

Fig. S19 PI-ReTOF-MS ion signal for C_6H_nO (n = 4, 6, 8, 10, 12, 14) versus temperature subliming from carbon monoxide-acetylene ($CO–C_2H_2$; $C^{18}O–C_2D_2$) ices.

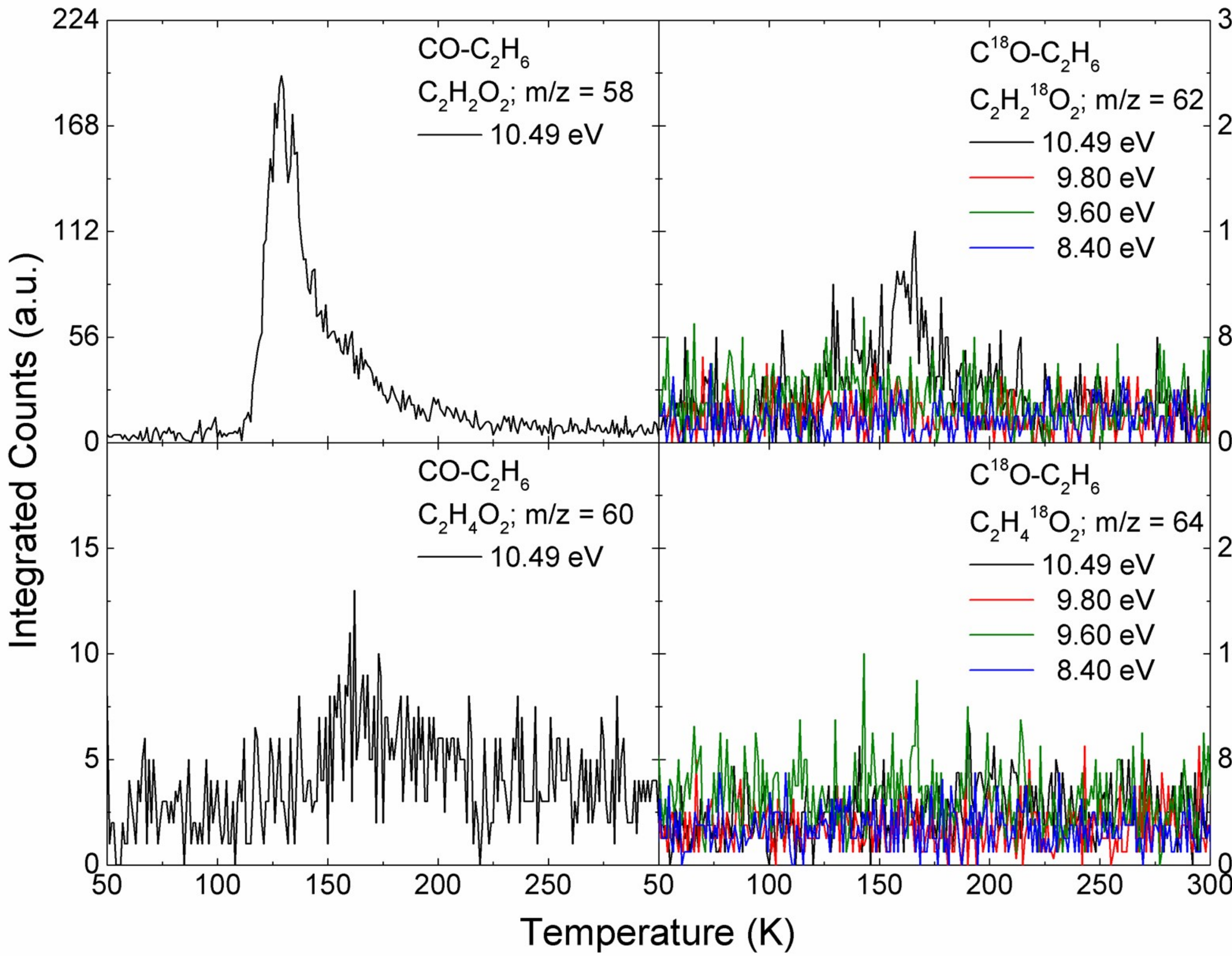

Fig. S20 PI-ReTOF-MS ion signal for $C_2H_nO_2$ (n = 2, 4) versus temperature subliming from carbon monoxide-ethane ($CO–C_2H_6$; $C^{18}O–C_2H_6$) ices.

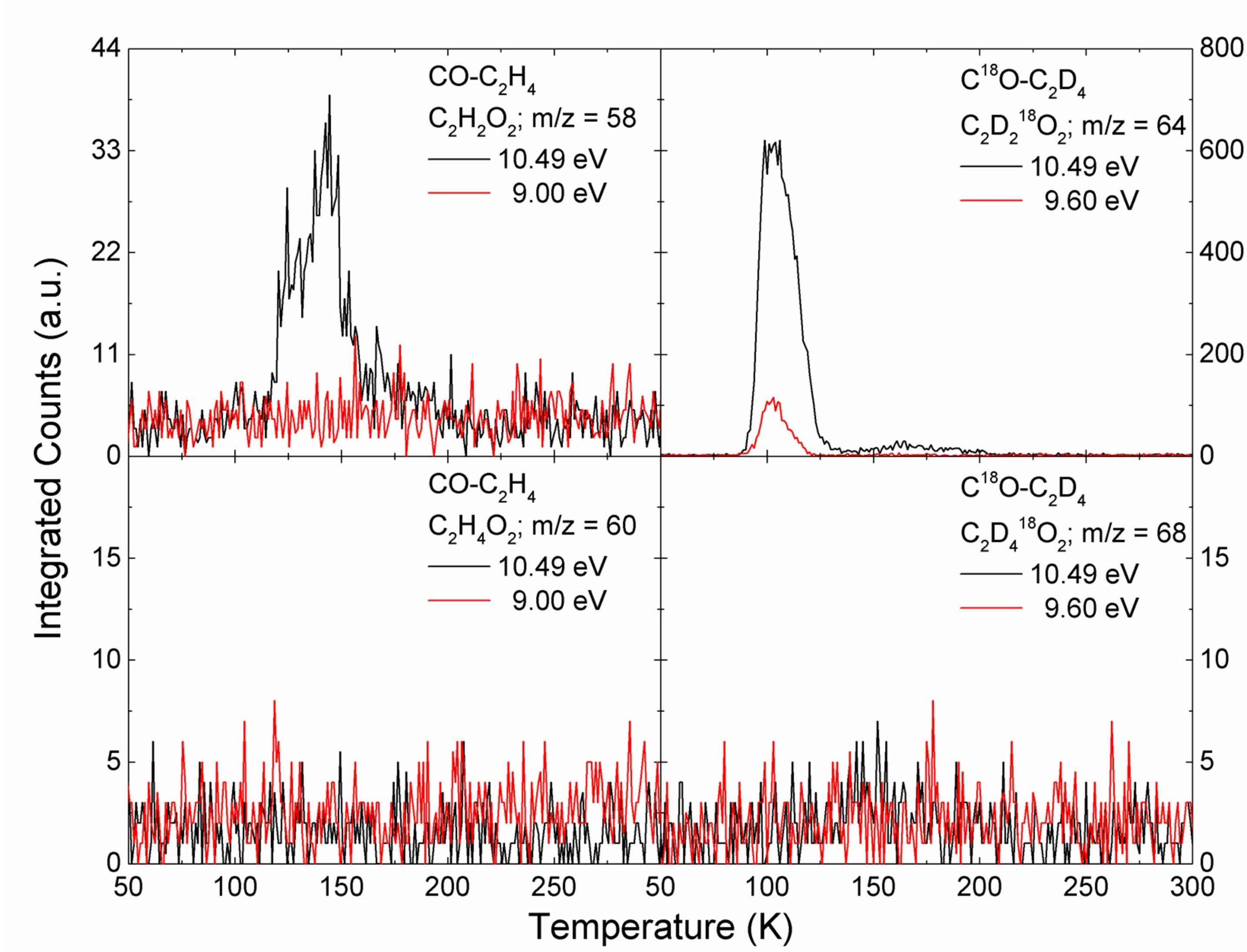

Fig. S21 PI-ReTOF-MS ion signal for $C_2H_nO_2$ (n = 2, 4) versus temperature subliming from carbon monoxide-ethylene (CO–C_2H_4; $C^{18}O$–C_2D_4) ices.

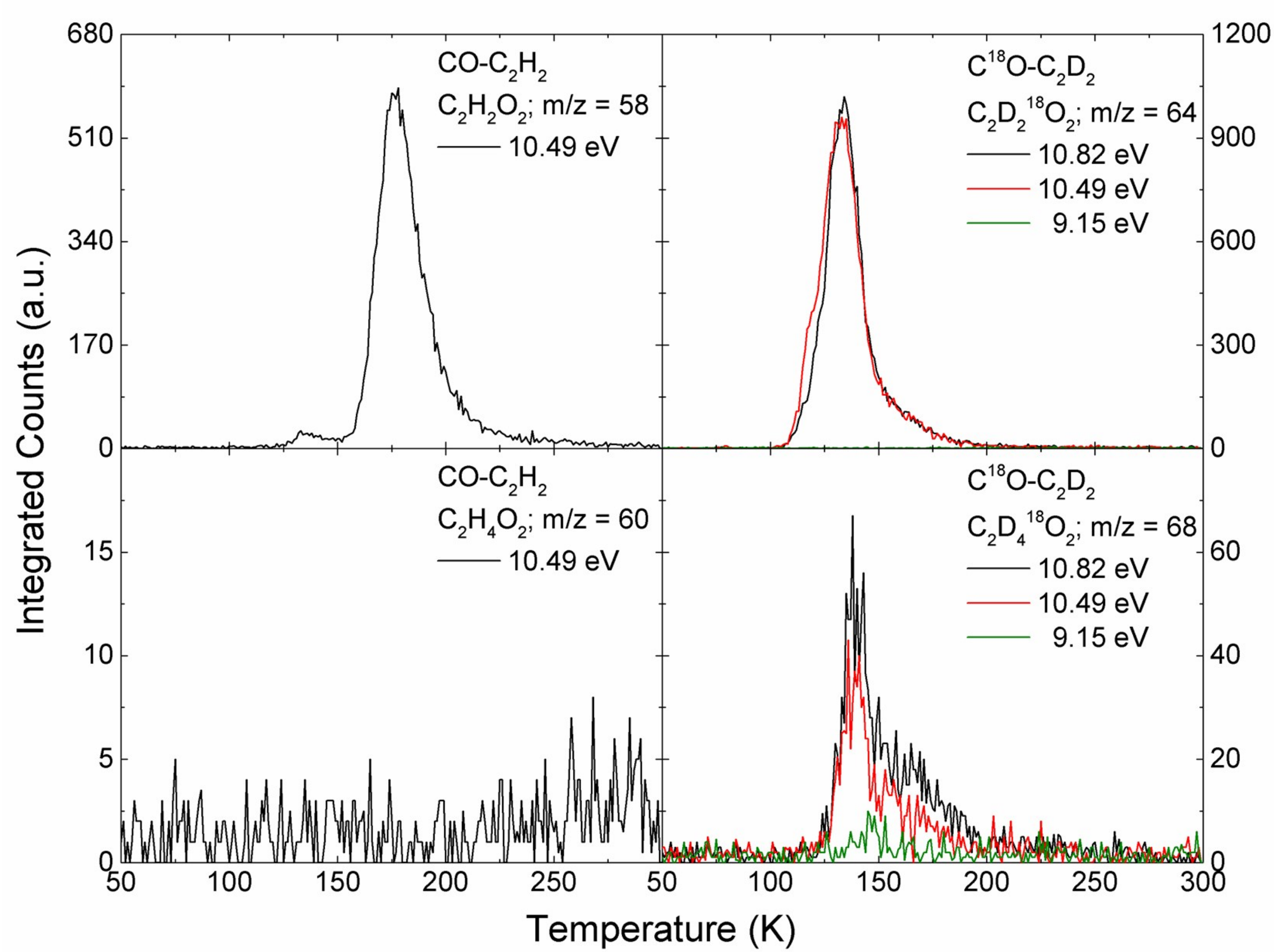

Fig. S22 PI-ReTOF-MS ion signal for $C_2H_nO_2$ (n = 2, 4) versus temperature subliming from carbon monoxide-acetylene (CO–C_2H_2; $C^{18}O$–C_2D_2) ices.

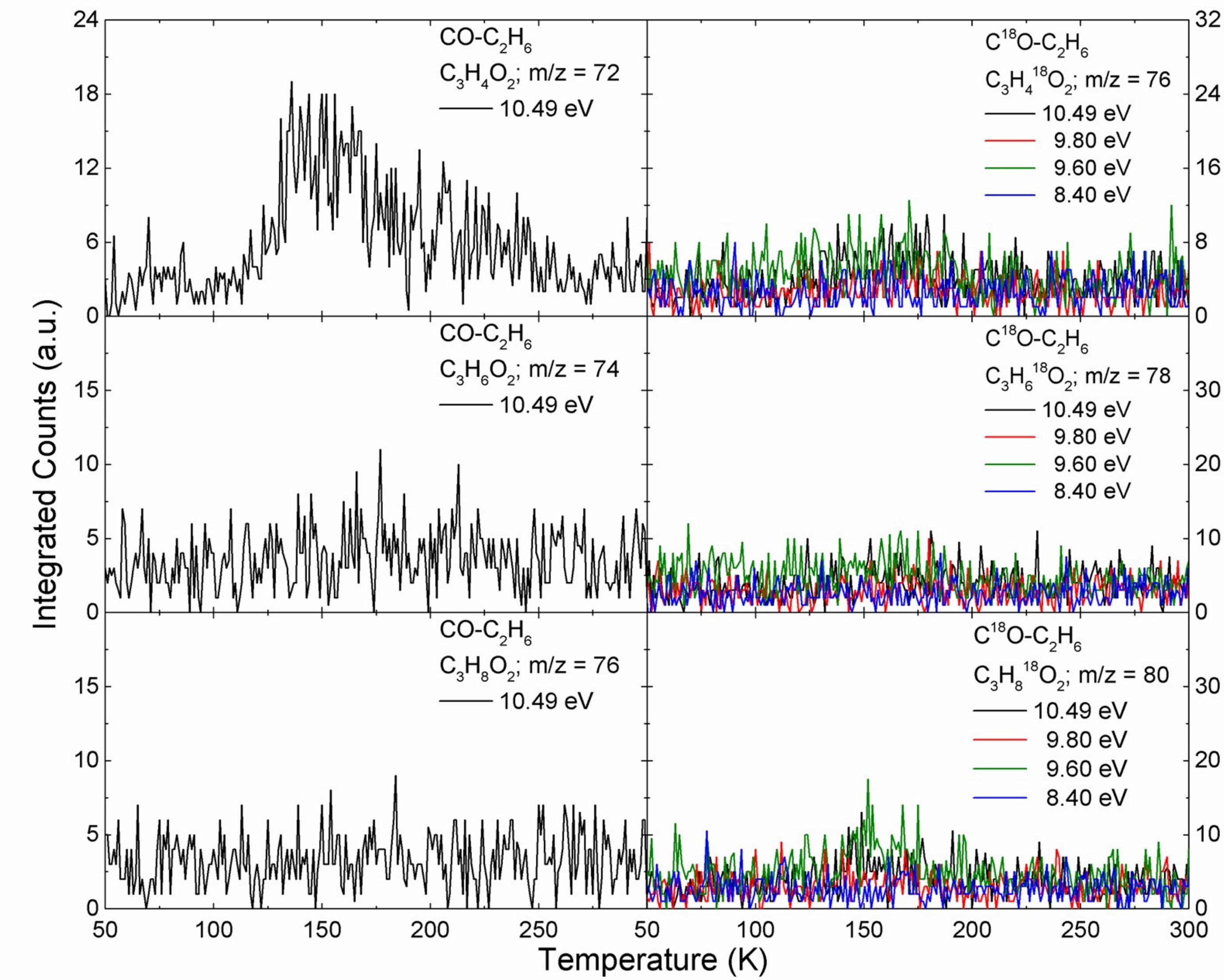

Fig. S23 PI-ReTOF-MS ion signal for $C_3H_nO_2$ (n = 4, 6, 8) versus temperature subliming from carbon monoxide-ethane (CO–C_2H_6; $C^{18}O$–C_2H_6) ices.

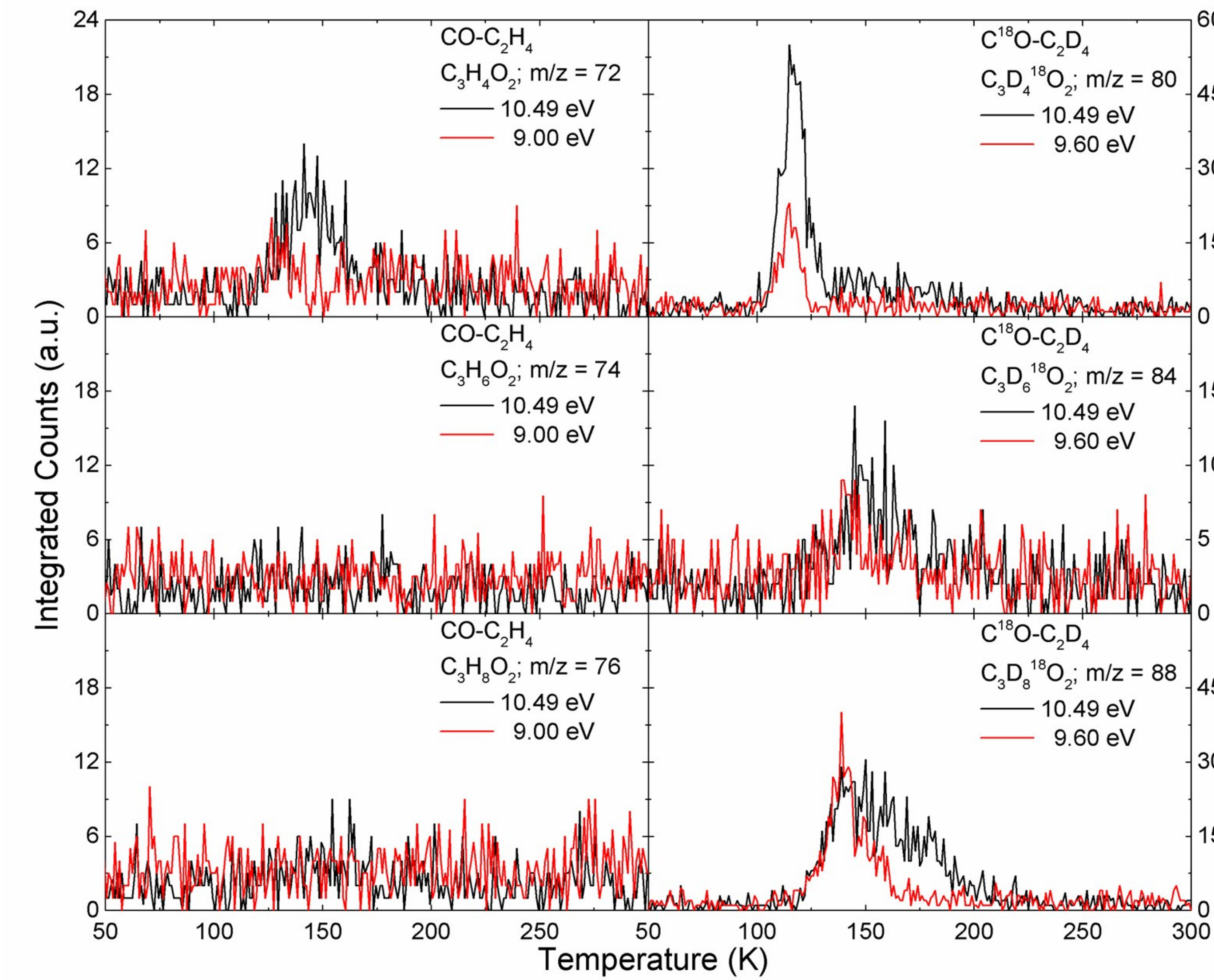

Fig. S24 PI-ReTOF-MS ion signal for $C_3H_nO_2$ (n = 4, 6, 8) versus temperature subliming from carbon monoxide-ethylene (CO–C_2H_4; $C^{18}O$–C_2D_4) ices.

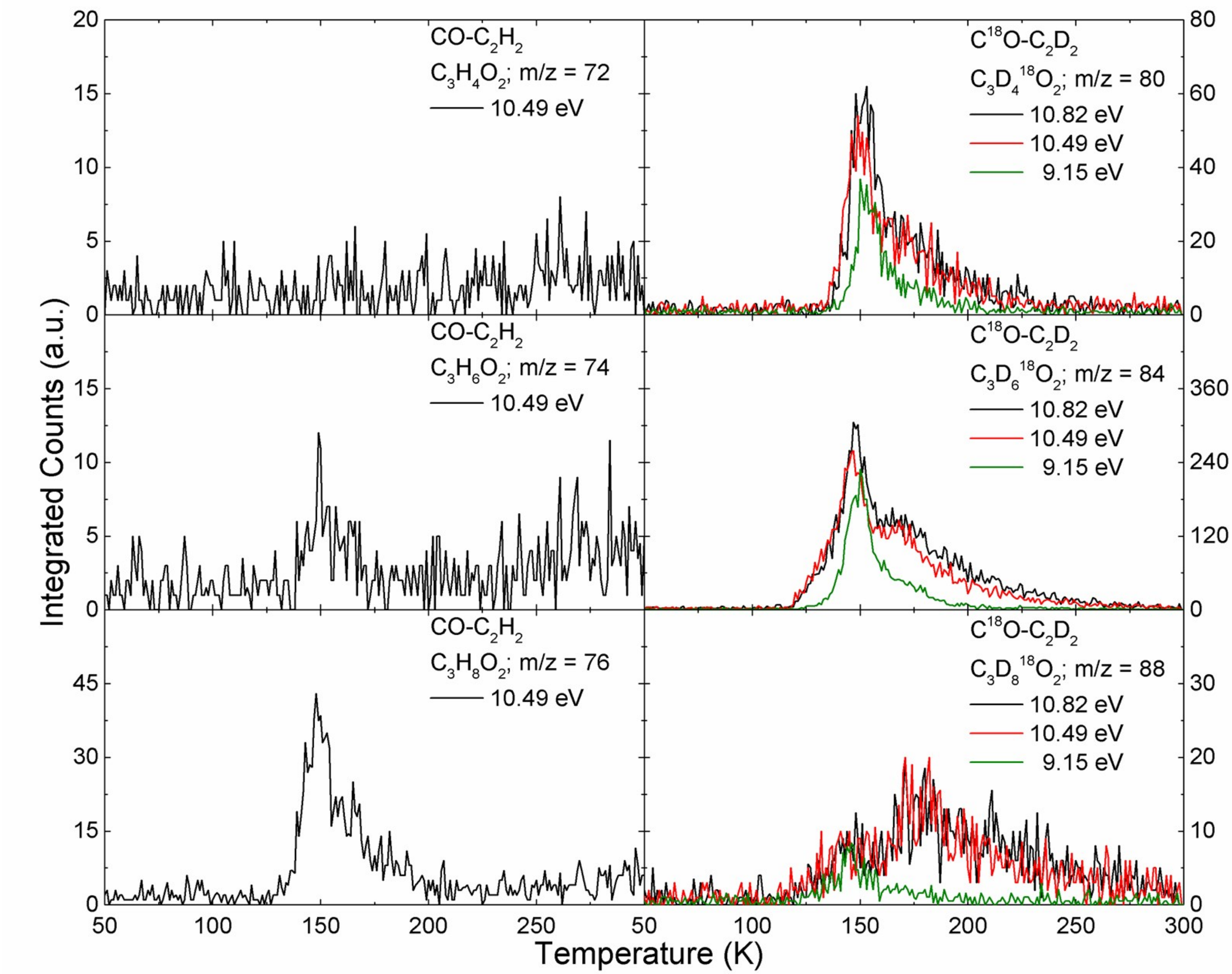

Fig. S25 PI-ReTOF-MS ion signal for $C_3H_nO_2$ (n = 4, 6, 8) versus temperature subliming from carbon monoxide-acetylene (CO–C_2H_2; $C^{18}O–C_2D_2$) ices.

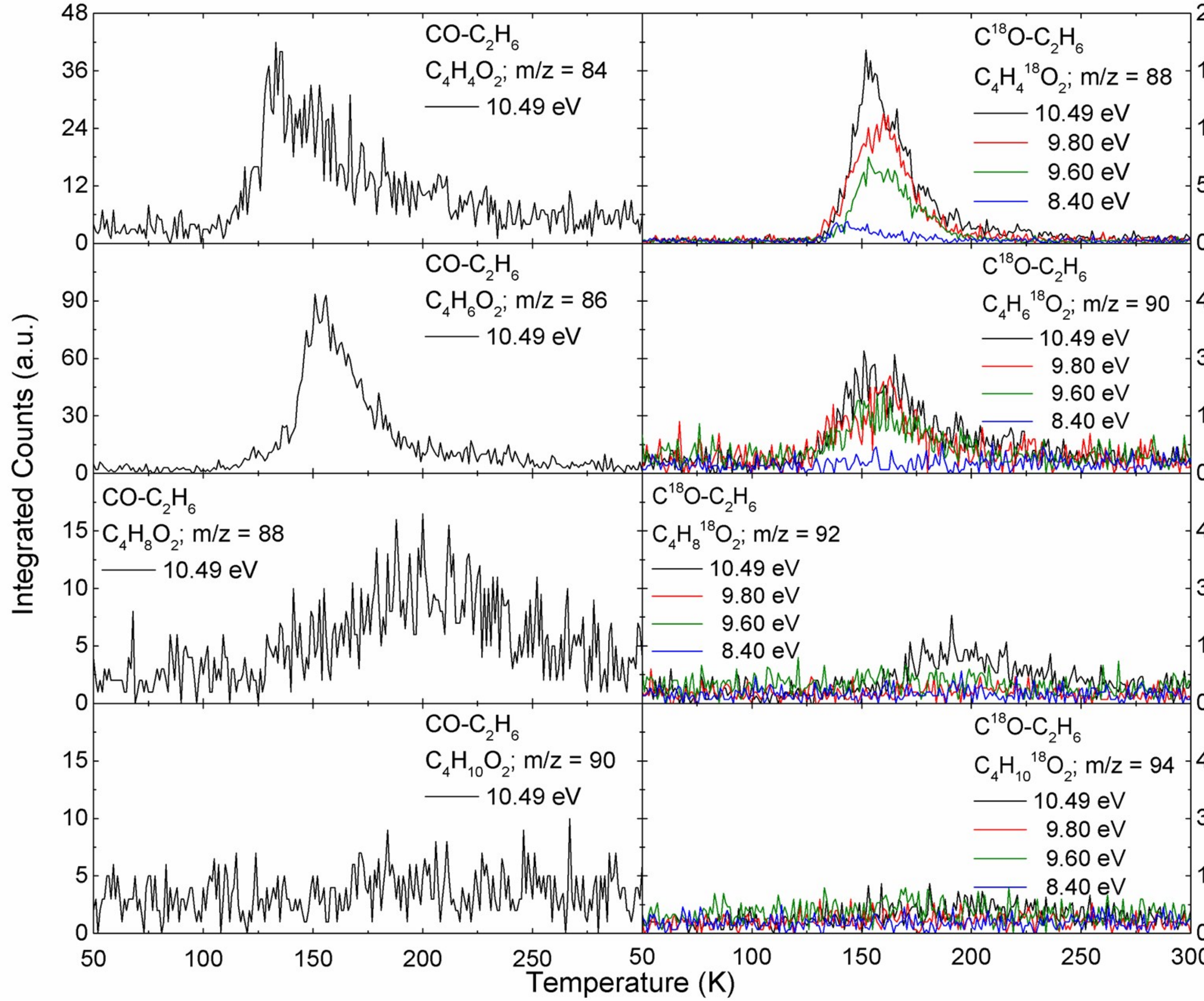

Fig. S26 PI-ReTOF-MS ion signal for $C_4H_nO_2$ (n = 4, 6, 8, 10) versus temperature subliming from carbon monoxide-ethane (CO–C_2H_6; $C^{18}O$–C_2H_6) ices.

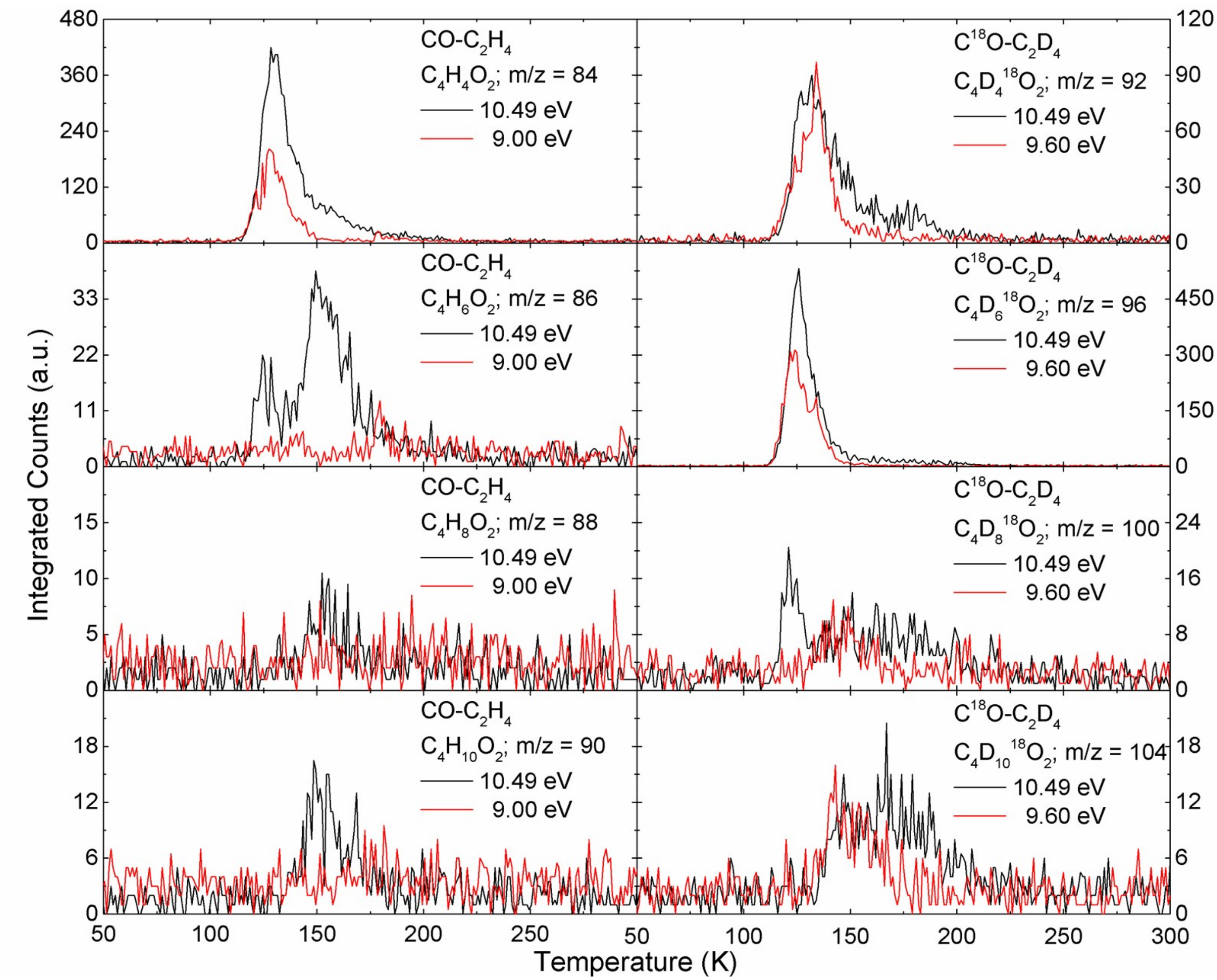

Fig. S27 PI-ReTOF-MS ion signal for $C_4H_nO_2$ (n = 4, 6, 8, 10) versus temperature subliming from carbon monoxide-ethylene (CO–C_2H_4; $C^{18}O$–C_2D_4) ices.

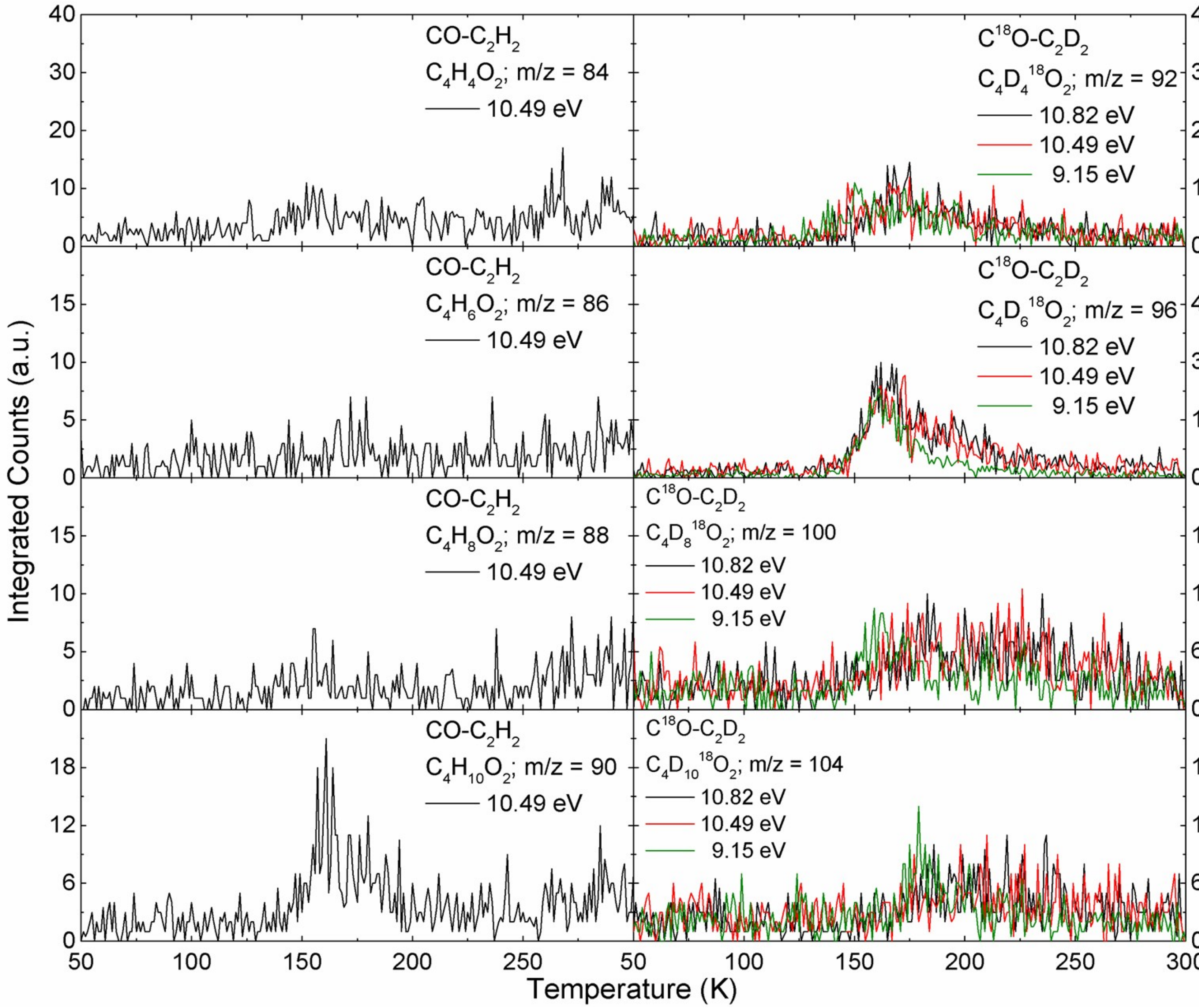

Fig. S28 PI-ReTOF-MS ion signal for $C_4H_nO_2$ (n = 4, 6, 8, 10) versus temperature subliming from carbon monoxide-acetylene (CO–C_2H_2; $C^{18}O–C_2D_2$) ices.

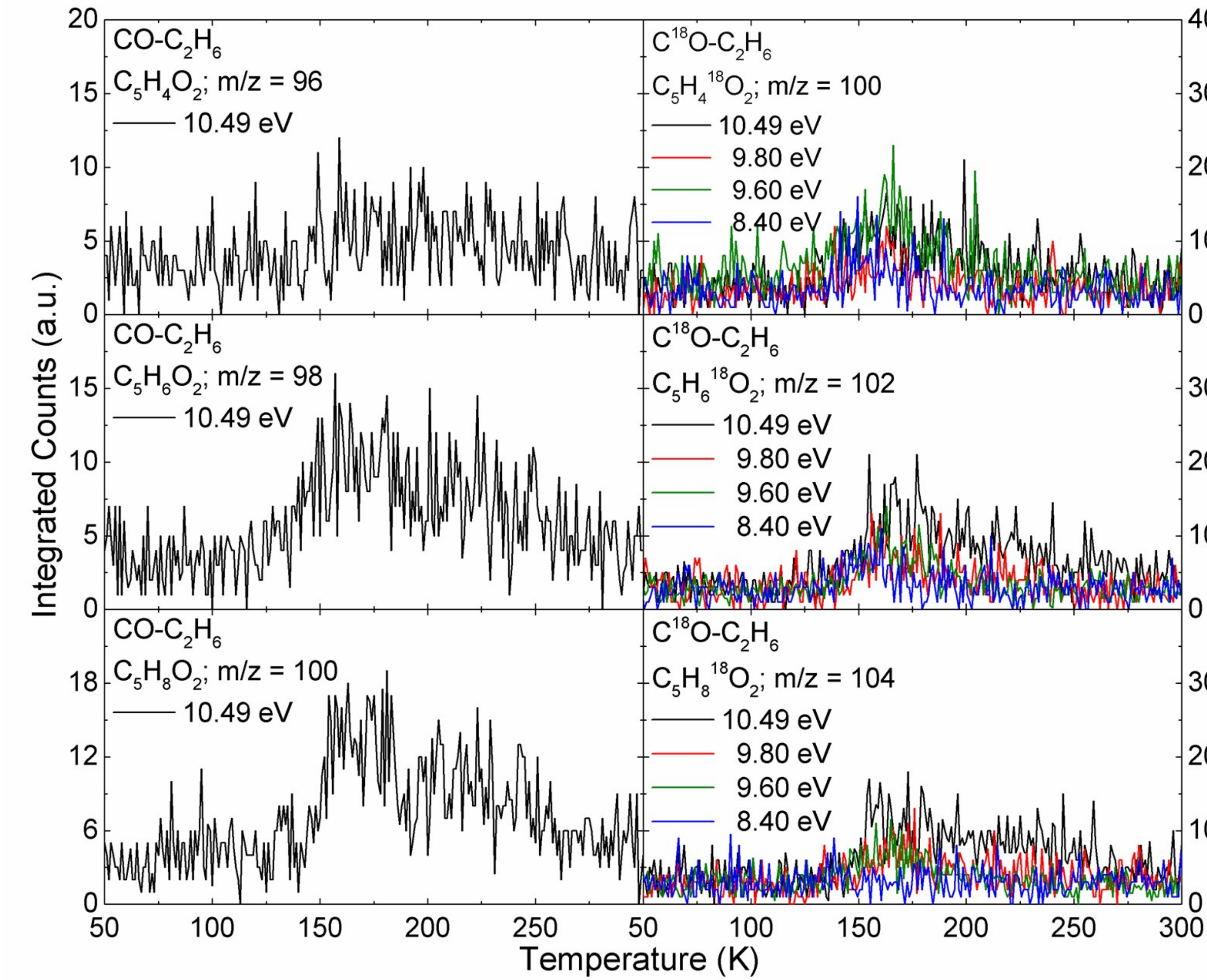

Fig. S29 PI-ReTOF-MS ion signal for $C_5H_nO_2$ (n = 6, 8) versus temperature subliming from carbon monoxide-ethane ($CO–C_2H_6$; $C^{18}O–C_2H_6$) ices.

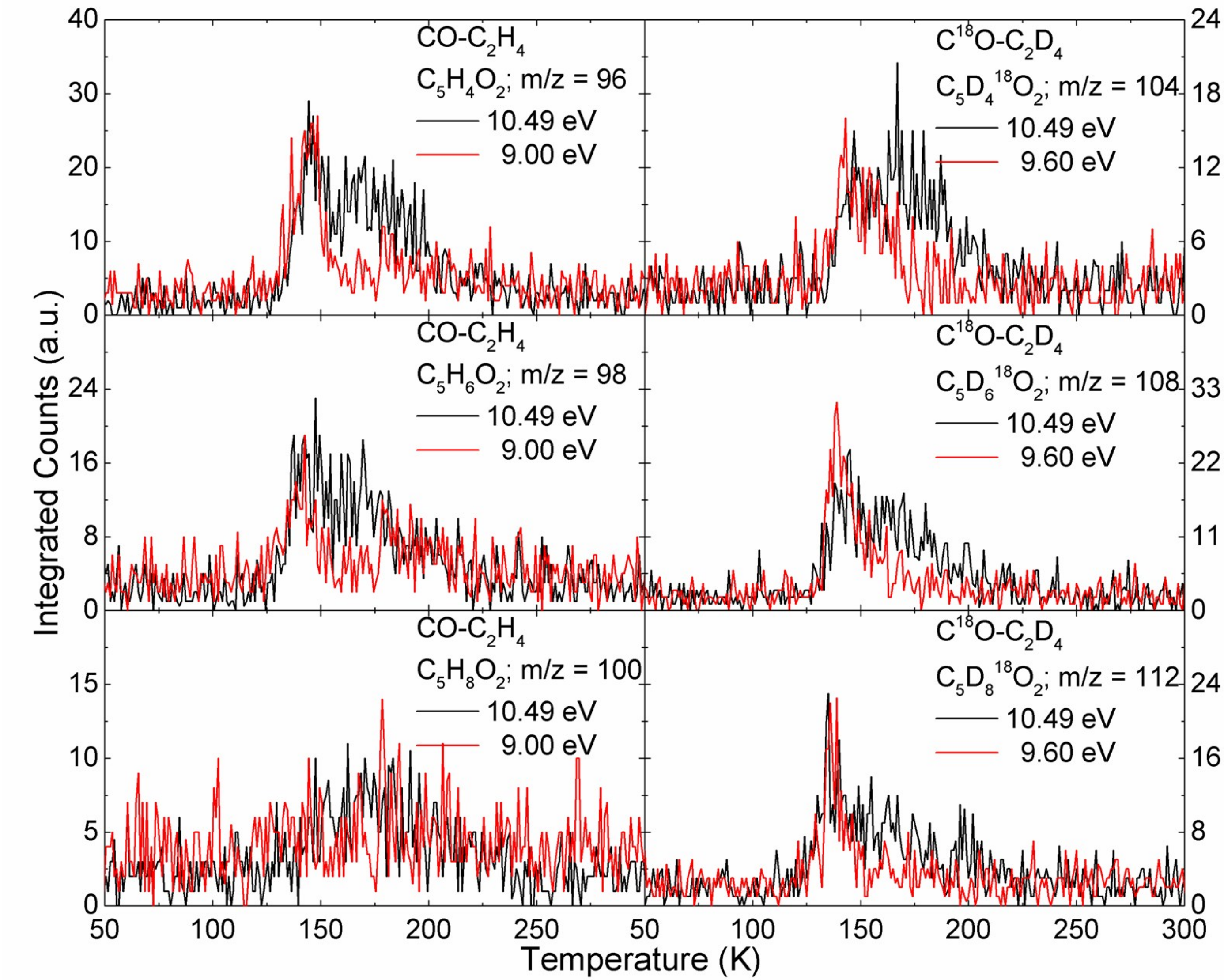

Fig. S30 PI-ReTOF-MS ion signal for $C_5H_nO_2$ (n = 6, 8) versus temperature subliming from carbon monoxide-ethylene ($CO–C_2H_4$; $C^{18}O–C_2D_4$) ices.

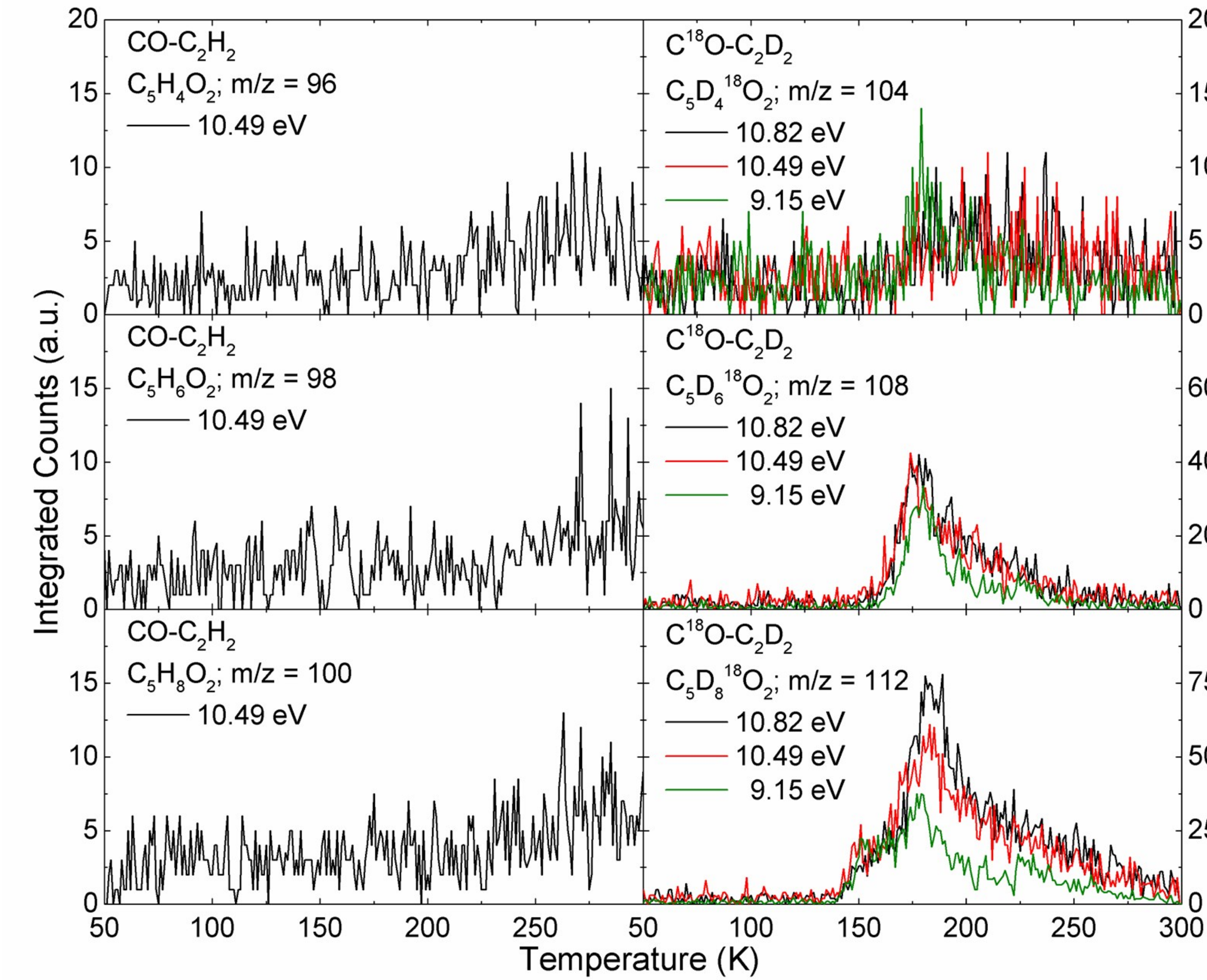

Fig. S31 PI-ReTOF-MS ion signal for $C_5H_nO_2$ (n = 6, 8) versus temperature subliming from carbon monoxide-acetylene ($CO–C_2H_2$; $C^{18}O–C_2D_2$) ices.

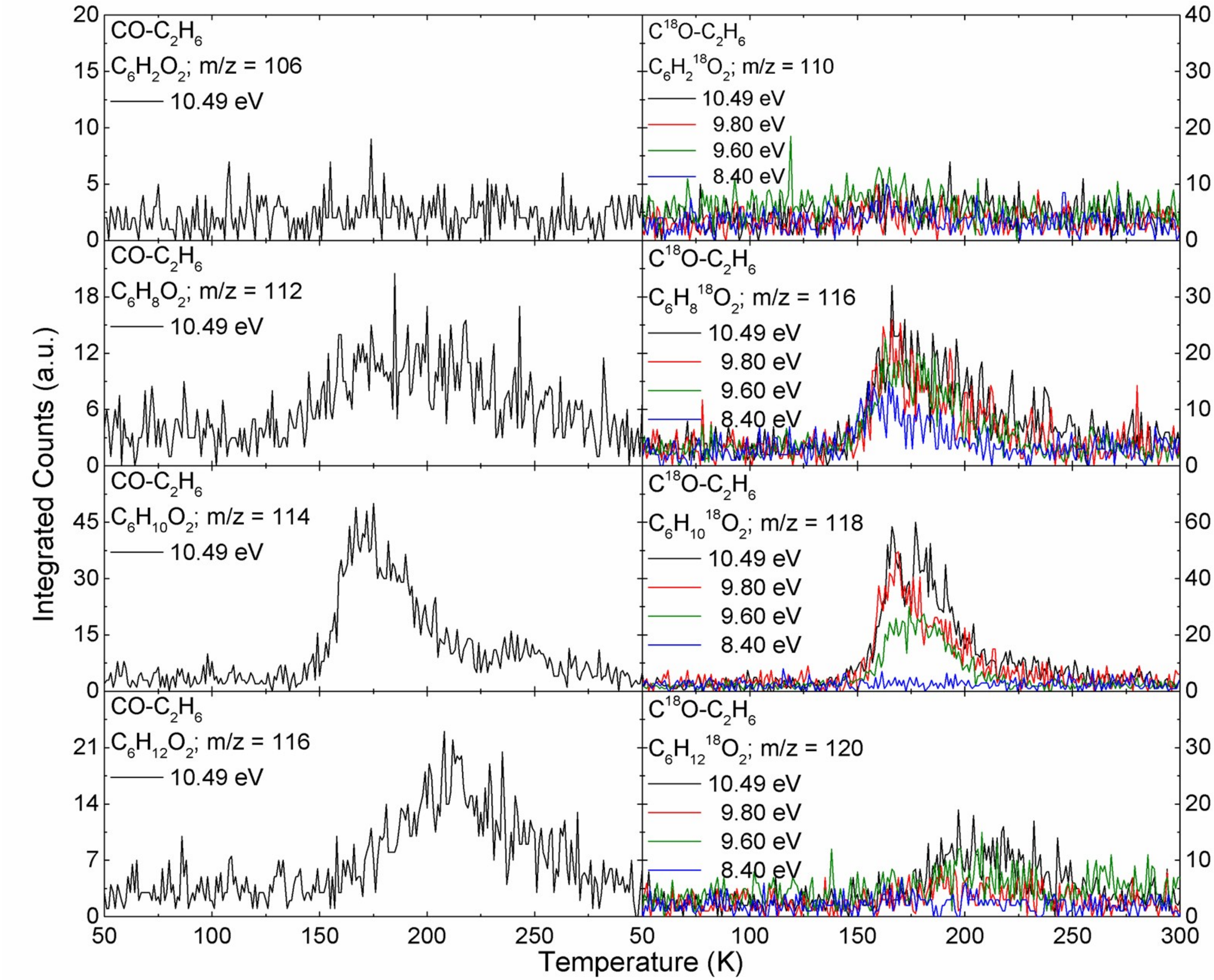

Fig. S32 PI-ReTOF-MS ion signal for $C_6H_nO_2$ (n = 8, 10, 12) versus temperature subliming from carbon monoxide-ethane ($CO–C_2H_6$; $C^{18}O–C_2H_6$) ices.

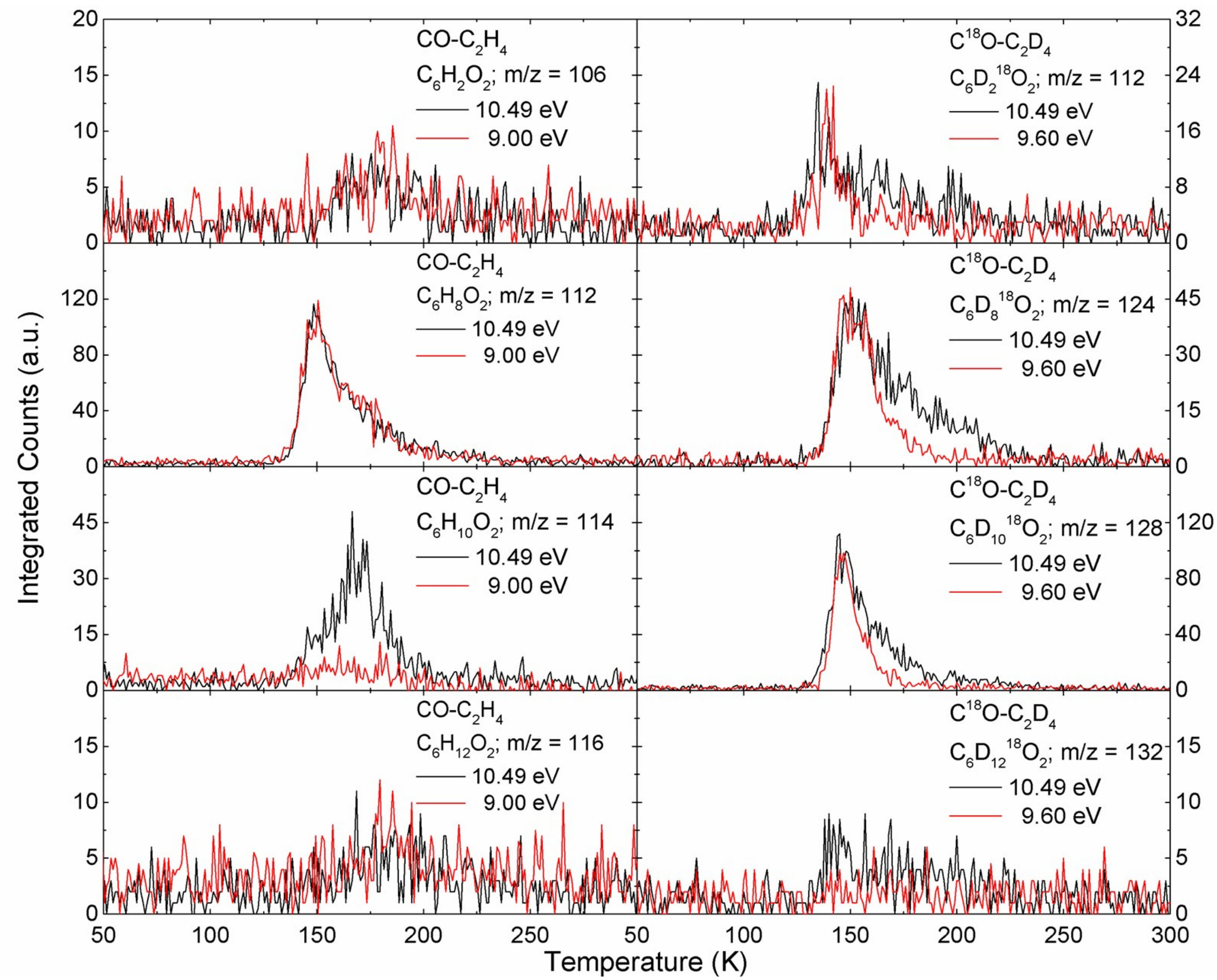

Fig. S33 PI-ReTOF-MS ion signal for $C_6H_nO_2$ (n = 8, 10, 12) versus temperature subliming from carbon monoxide-ethylene (CO–C_2H_4; $C^{18}O$–C_2D_4) ices.

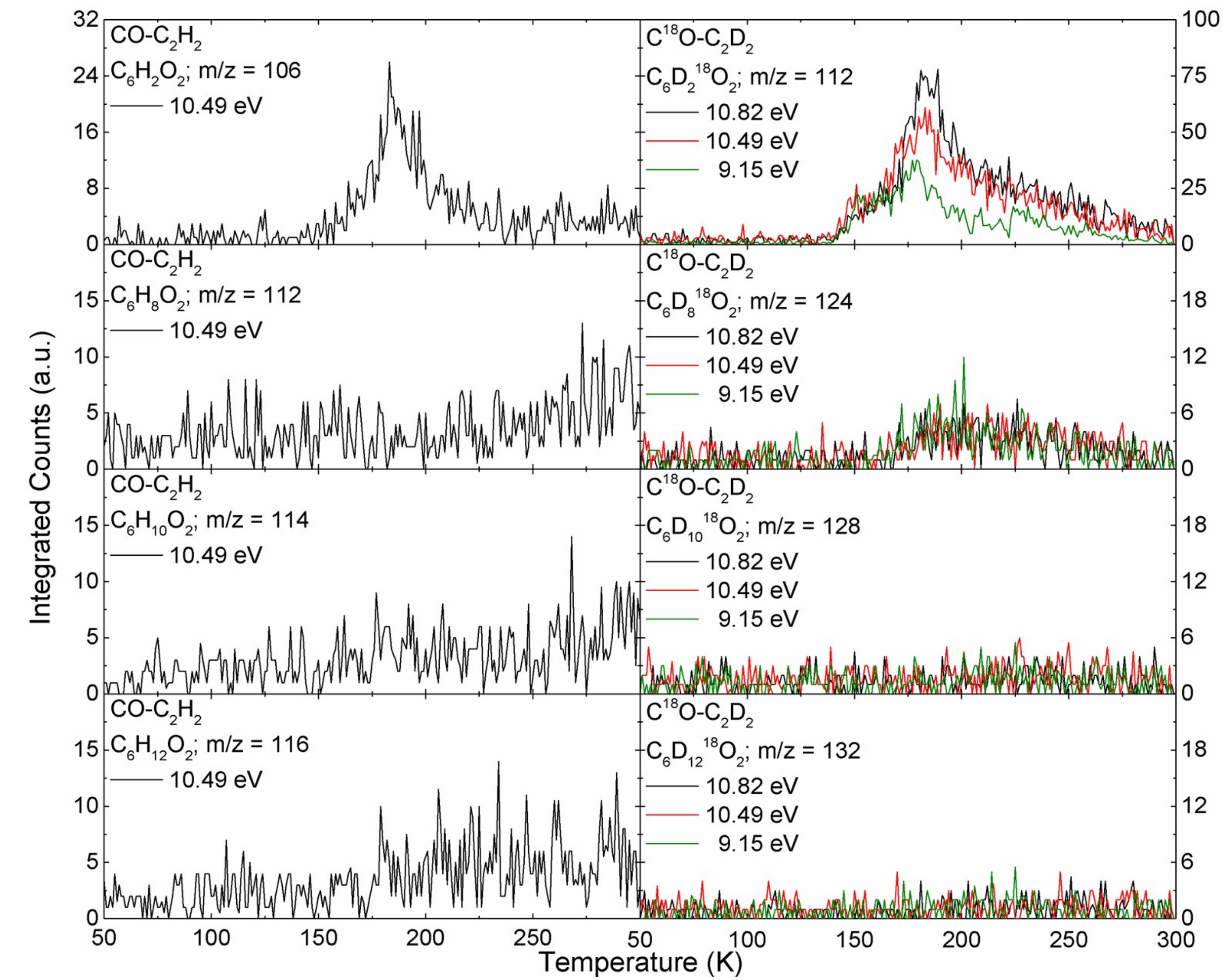

Fig. S34 PI-ReTOF-MS ion signal for $C_6H_nO_2$ (n = 8, 10, 12) versus temperature subliming from carbon monoxide-acetylene (CO–C_2H_2; $C^{18}O$–C_2D_2) ices.

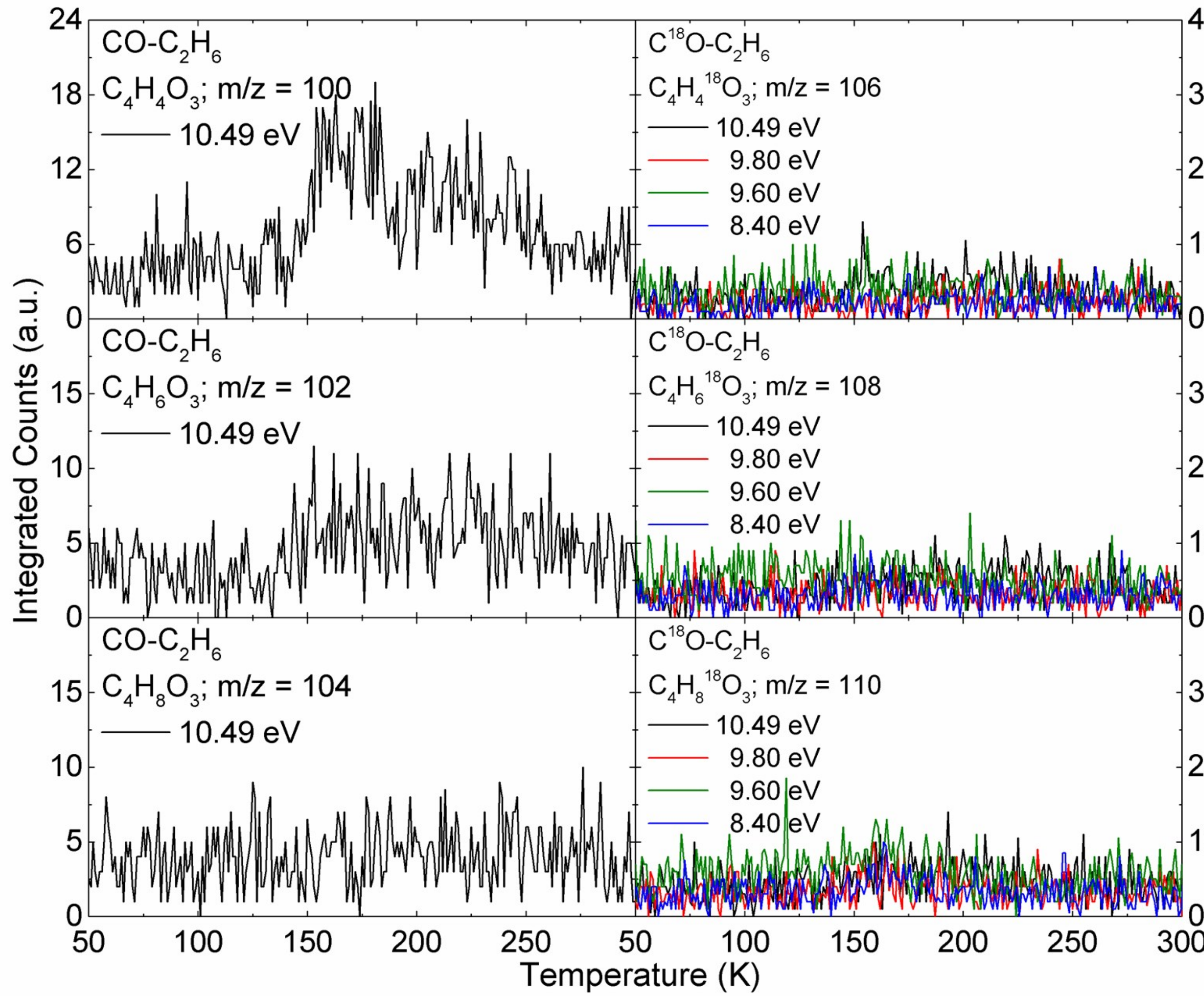

Fig. S35 PI-ReTOF-MS ion signal for $C_4H_nO_3$ (n = 4, 6, 8) versus temperature subliming from carbon monoxide-ethane ($CO–C_2H_6$; $C^{18}O–C_2H_6$) ices.

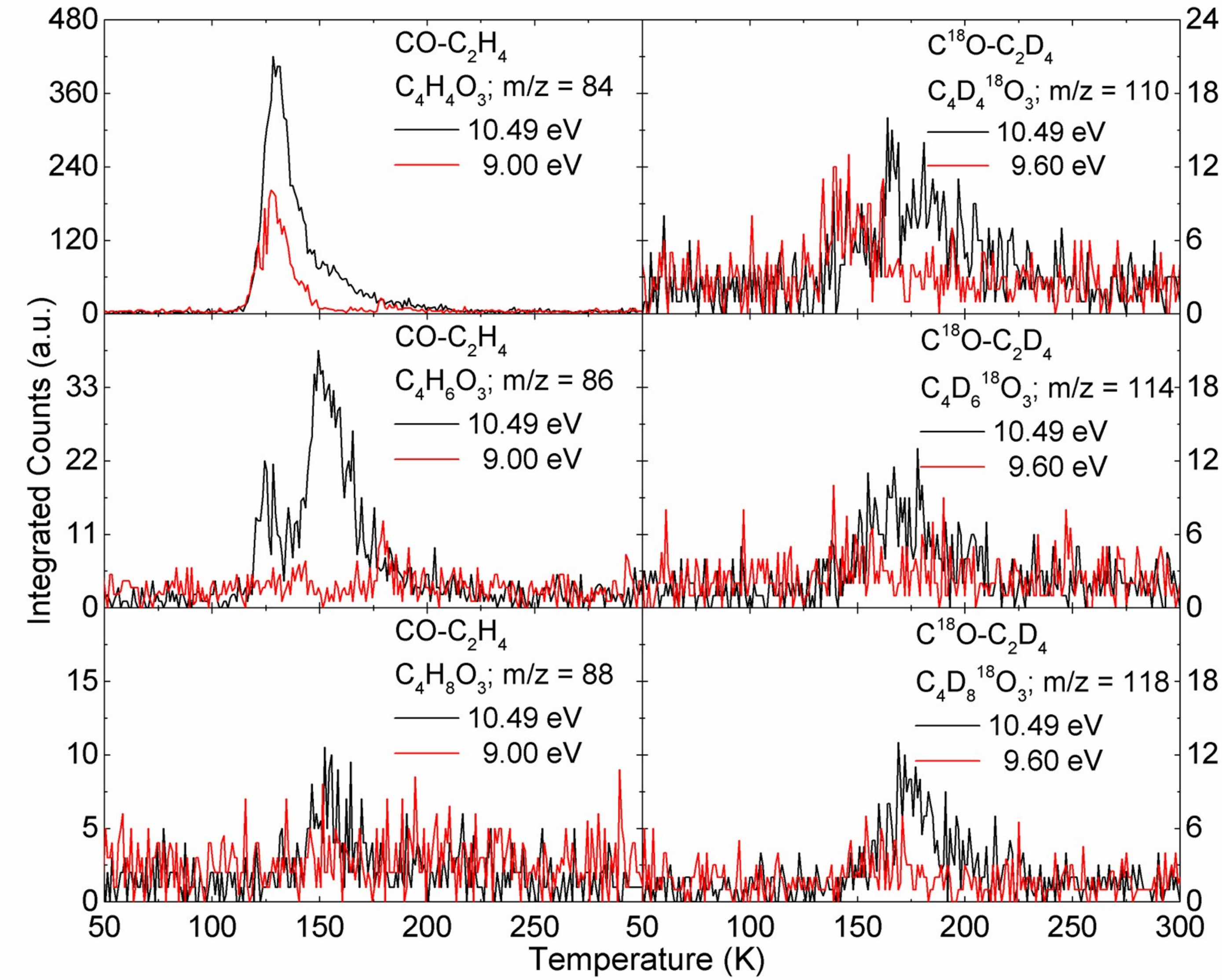

Fig. S36 PI-ReTOF-MS ion signal for $C_4H_nO_3$ (n = 4, 6, 8) versus temperature subliming from carbon monoxide-ethylene ($CO–C_2H_4$; $C^{18}O–C_2D_4$) ices.

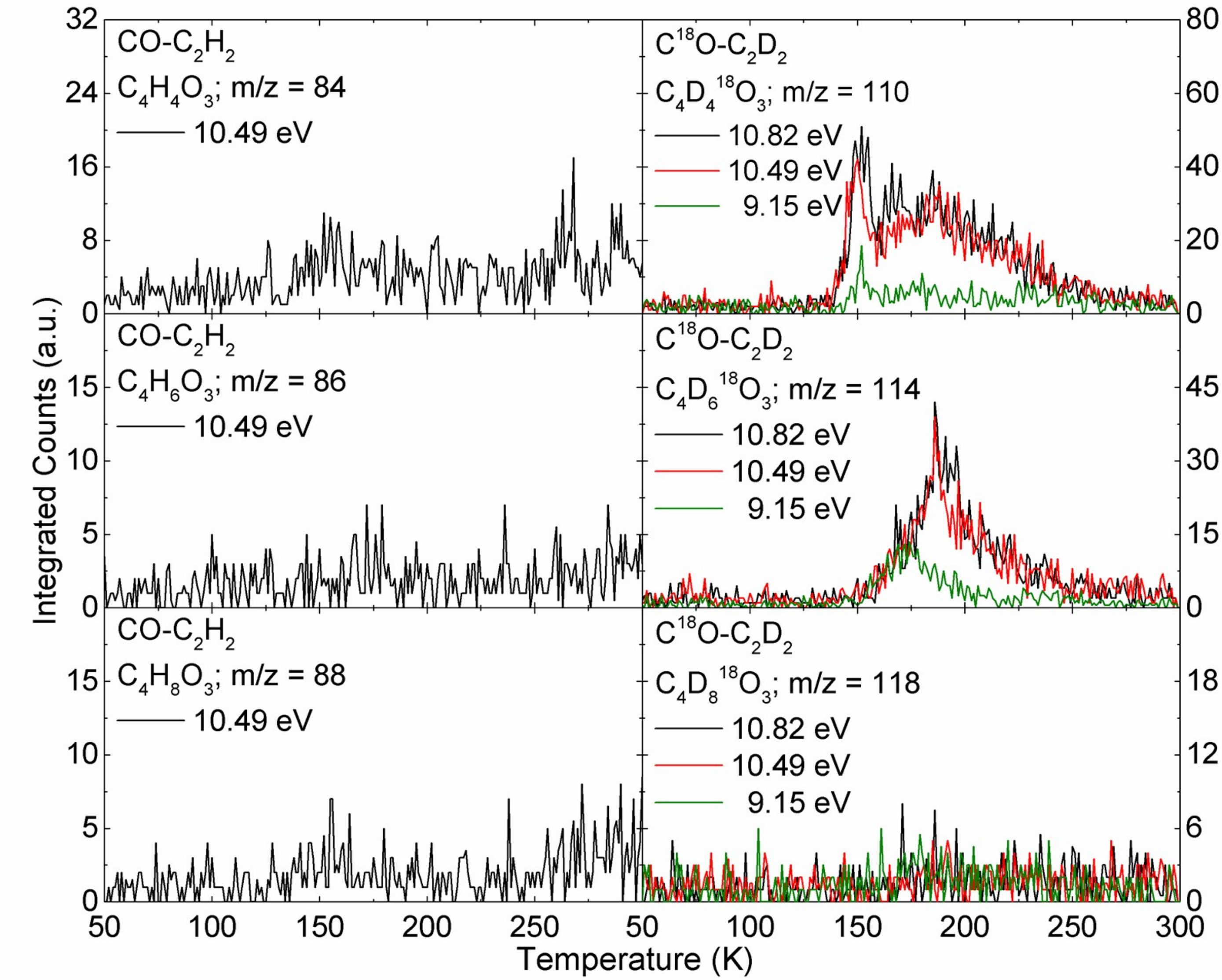

Fig. S37 PI-ReTOF-MS ion signal for $C_4H_nO_3$ (n = 4, 6, 8) versus temperature subliming from carbon monoxide-acetylene (CO–C_2H_2; $C^{18}O$–C_2D_2) ices.

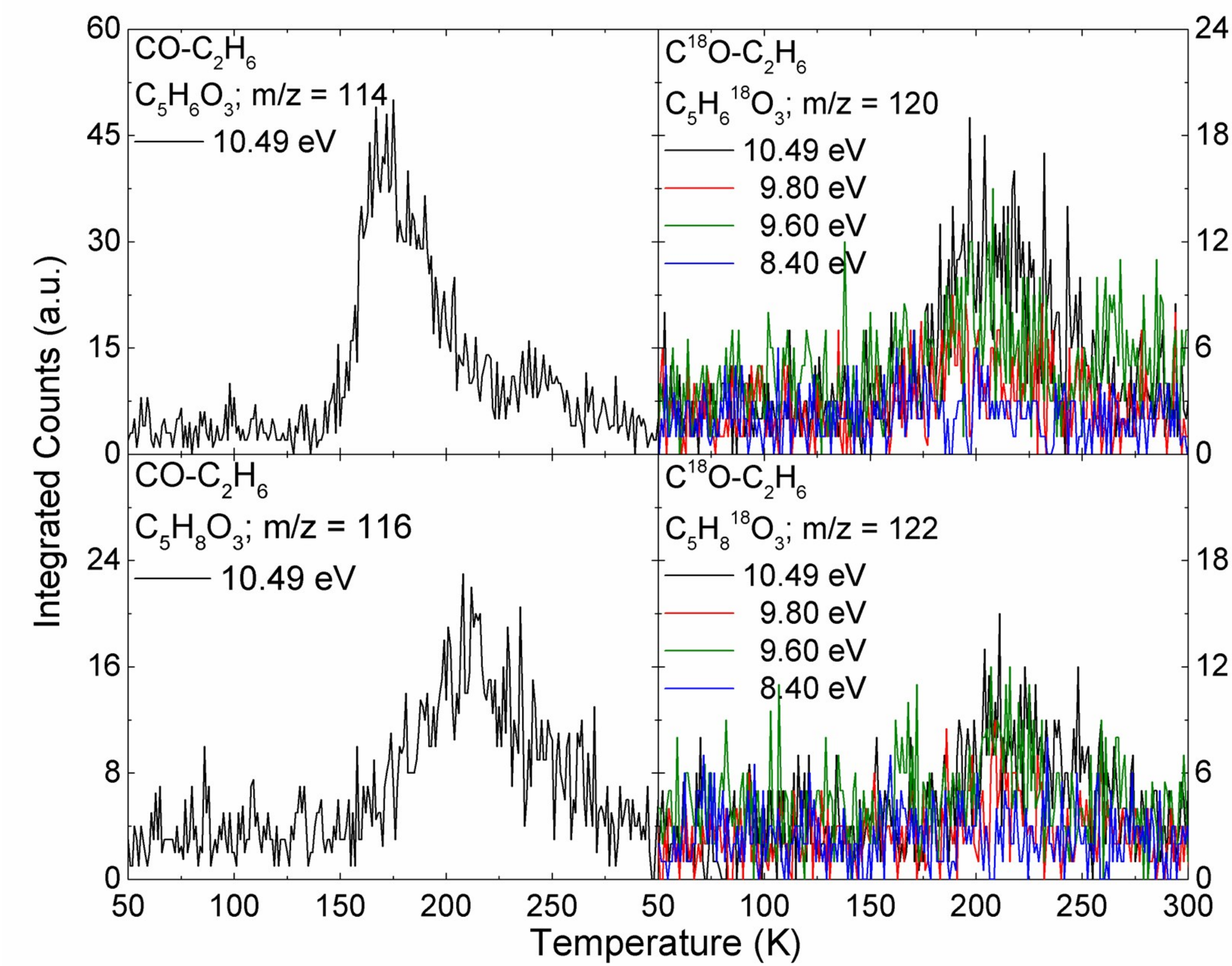

Fig. S38 PI-ReTOF-MS ion signal for $C_5H_nO_3$ (n = 6, 8) versus temperature subliming from carbon monoxide-ethane (CO–C_2H_6; $C^{18}O$–C_2H_6) ices.

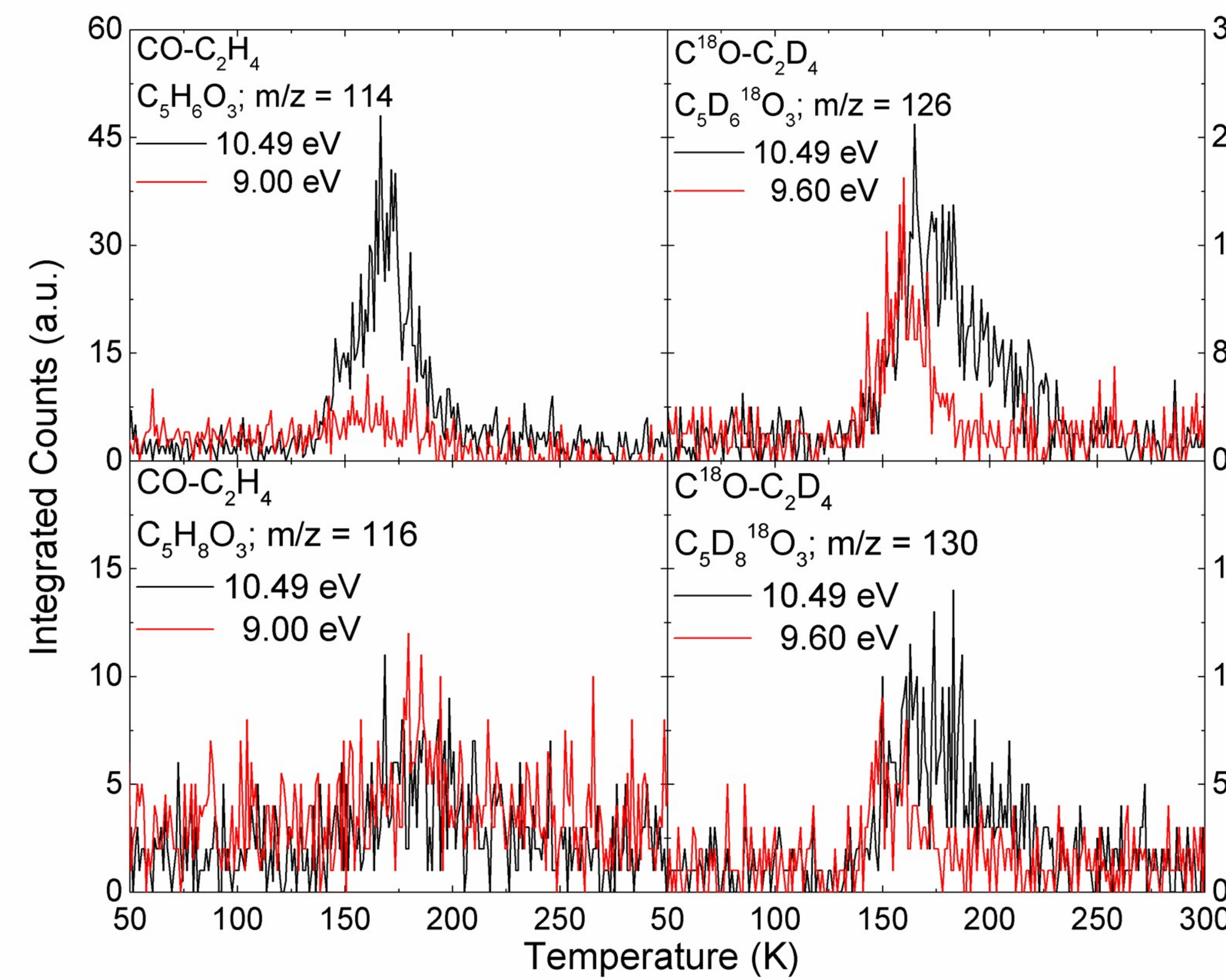

Fig. S39 PI-ReTOF-MS ion signal for $C_5H_nO_3$ (n = 6, 8) versus temperature subliming from carbon monoxide-ethylene ($CO–C_2H_4$; $C^{18}O–C_2D_4$) ices.

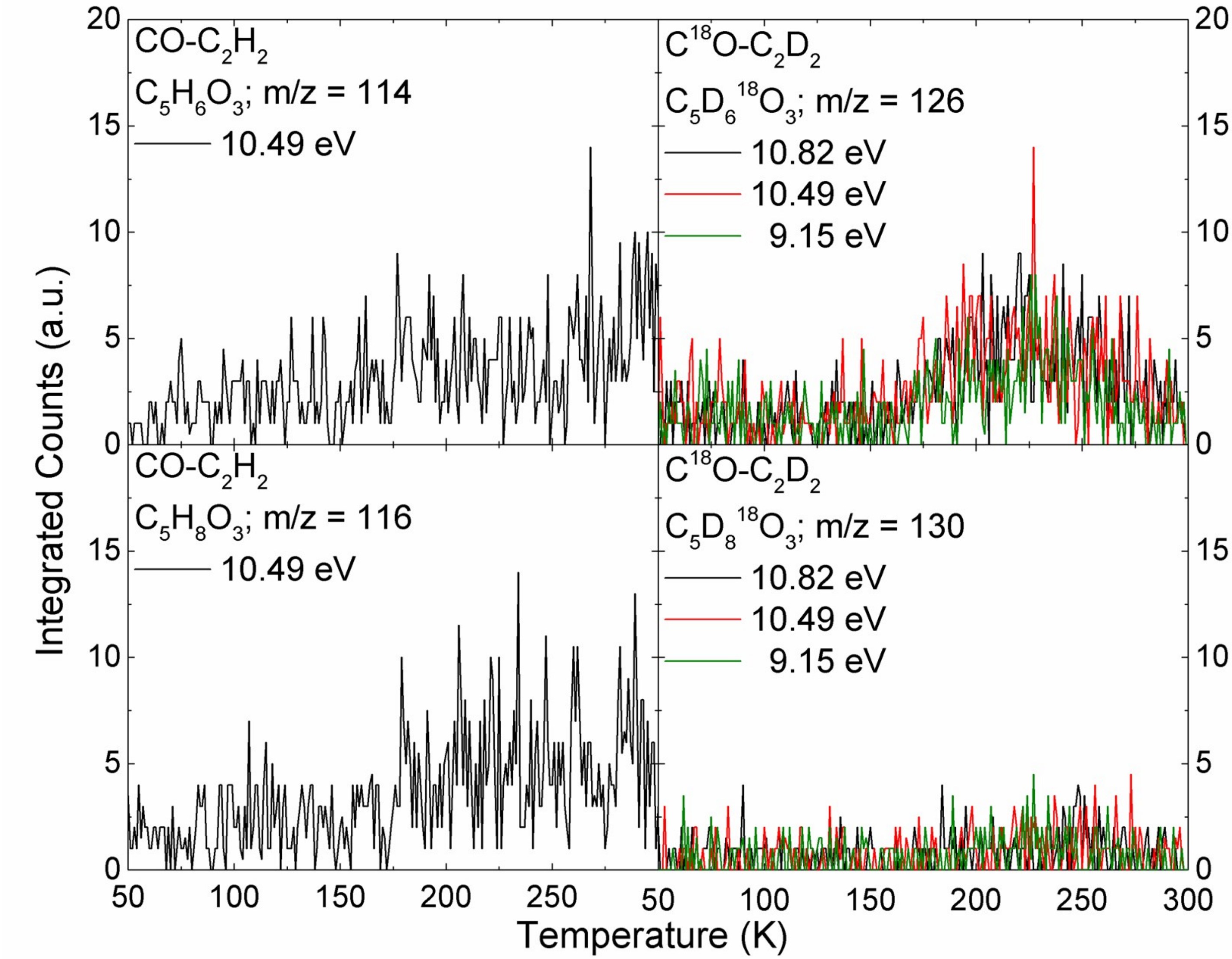

Fig. S40 PI-ReTOF-MS ion signal for $C_5H_nO_3$ (n = 6, 8) versus temperature subliming from carbon monoxide-acetylene (CO–C_2H_2; $C^{18}O$–C_2D_2) ices.

References and Notes

1. R. L. Hudson, R. F. Ferrante and M. H. Moore, *Icarus*, 2014, **228**, 276-287.
2. C. S. Jamieson, A. M. Mebel and R. I. Kaiser, *Astrophys. J., Sup.*, 2006, **163**, 184-206.
3. W. Gallaway and E. Barker, *J. Chem. Phys.*, 1942, **10**, 88-97.
4. M. J. Abplanalp and R. I. Kaiser, *Astrophys. J.*, 2017, **836**, 195-226.
5. M. J. Abplanalp and R. I. Kaiser, *Astrophys. J.*, 2016, **827**, 132-161.
6. M. J. Abplanalp, S. Góbi, A. Bergantini, A. M. Turner and R. I. Kaiser, *ChemPhysChem*, 2018, **19**, 556-560.
7. M. J. Abplanalp, S. Gozem, A. I. Krylov, C. N. Shingledecker, E. Herbst and R. I. Kaiser, *Proc. Natl. Acad. Sci. U. S. A.*, 2016, **113**, 7727-7732.
8. M. J. Abplanalp, A. Borsuk, B. M. Jones and R. I. Kaiser, *Astrophys. J.*, 2015, **814**, 45-61.
9. G. L. Bottger and D. F. E. Jr., *J. Chem. Phys.*, 1964, **40**, 2010-2017.
10. C. J. Bennett, C. S. Jamieson, Y. Osumura and R. I. Kaiser, *Astrophys. J.*, 2006, **653**, 792-811.
11. J. He, K. Gao, G. Vidali, C. J. Bennett and R. I. Kaiser, *Astrophys. J.*, 2010, **721**, 1656.
12. P. Calvani, S. Lupi and P. Maselli, *J. Chem. Phys.*, 1989, **91**, 6737-6742.
13. M. J. Abplanalp, B. M. Jones and R. I. Kaiser, *Phys. Chem. Chem. Phys.*, 2018, **20**, 5435-5468.
14. Y.-J. Wu and B.-M. Cheng, *Chem. Phys. Lett.*, 2008, **461**, 53-57.
15. E. Tørneng, C. J. Nielsen, P. Klaeboe, H. Hopf and H. Priebe, *Spectrochim. Acta A*, 1980, **36**, 975-987.
16. P. A. Gerakines, W. A. Schutte, J. M. Greenberg and E. F. van Dishoeck, *Astron. Astrophys.*, 1995, **296**, 810-818.
17. R. I. Kaiser and K. Roessler, *Astrophys. J.*, 1998, **503**, 959-975.
18. I. M. Nyquist, I. M. Mills, W. B. Person and B. Crawford, *J. Chem. Phys.*, 1957, **26**, 552-558.
19. M. G. Wisnosky, D. F. Eggers, L. R. Fredrickson and J. C. Decius, *J. Chem. Phys.*, 1983, **79**, 3513-3516.
20. S. B. Tejada and D. F. Eggers, *Spectrochim Acta A*, 1976, **32**, 1557-1562.
21. M. E. Jacox, *J. Chem. Phys.*, 1962, **36**, 140-143.
22. S. Kondo and S. Saëki, *Spectrochim. Acta A*, 1973, **29**, 735-751.
23. R. I. Kaiser, S. Maity and B. M. Jones, *Phys. Chem. Chem. Phys.*, 2014, **16**, 3399-3424.